SCAFFOLD-FREE TRACHEAL CARTILAGE ENGINEERING USING ROLLER BOTTLE CULTURE

by

Imran R. Sheikh, B. Eng

Ryerson University, 2014

A thesis presented to Ryerson University

in partial fulfilment of the

requirement for the degree of

Master of Applied Science

in the Program of

Chemical Engineering

Toronto, Ontario, Canada, 2017

©Imran R. Sheikh 2017

Author's Declaration

I hereby declare that I am the sole author of this thesis. This is a true copy of the thesis, including any required final revisions, as accepted by my examiners.

I authorize Ryerson University to lend this thesis to other institutions or individuals for the purpose of scholarly research.

I further authorize Ryerson University to reproduce this thesis by photocopying or by other means, in total or in part, at the request of other institutions or individuals for the purpose of scholarly research.

I understand that my thesis may be made electronically available to the public.

Title: Scaffold-Free Tracheal Cartilage Engineering Using Roller Bottle Culture

Degree/Year: Master of Applied Science (MASc), 2017

Name: Imran Sheikh

Program: Chemical Engineering Graduate Program

University: Ryerson University

Abstract

Resection with primary anastomosis can only repair up to 50% of the adult trachea and up to 30% of the pediatric trachea when damaged. There is a strong clinical need for long-segment tracheal replacements. The goal of this research was to create a seamless, scaffold-free cartilage cylinder for tracheal tissue engineering *in vitro*. Primary bovine articular chondrocytes were seeded onto tracheal moulds for roller bottle culture and the effect of rotational speed, growth factor supplementation, and chondrocyte layering were investigated. After the 4-week culture period, samples were evaluated biochemically, histologically, and biomechanically. The results indicated that rotation was necessary for full tissue coverage, with slower rotational speeds generating thicker tissue with an improved extracellular matrix, IGF-1 supplementation generating thicker tissue rich in glycosaminoglycans with inferior mechanical properties, and chondrocyte layering producing thinner tissue with increased mechanical properties. Overall, scaffold-free tissue engineering can generate seamless cylindrical cartilage constructs using roller bottle culture for future applications in long-segment tracheal replacement.

Acknowledgements

I would like to thank Dr. Stephen Waldman for his guidance and mentorship, and for navigating me through the challenges of this project and encouraging my development as a scientist and as an engineer.

I would like to thank all my lab mates in the Waldman Lab: Dr. Johanna Weber, Dr. Lorraine Chiu, Kristina Collavino, Bethany Hughes, Omar Subedar, Olena Bojchuk, Roberto Tarantino, and Warren Tang. You made my time in the lab highly enjoyable and truly memorable.

I would like to thank my friends and family who always supported me when the challenge seemed insurmountable and kept me sane.

I would like to thank my mother, father, and sister for always being supportive and being my foundation in life.

Thank you all so much!

List of Tables

List of Figures

Table of Contents

1 Introduction

1.1 Clinical Need

Tracheal disorders arise from factors such as congenital malformations, cancer, infection, and prolonged intubation[1]. Congenital laryngotracheal malformations have an incidence of 1 in 100,000 [2], [3]; while tracheal cancer has an incidence of 1 in 500,000 [4]. Chronic airway stenosis has a mortality rate between 11–24 % [5]. Post-intubation tracheal stenosis is the most common reason for reconstructive airway surgeries with an incidence rate of 6-21% [6], [7]. Tracheal stenting can only remedy less acute disorders but suffers from infection, obstruction and integration problems [1], [3], [8]. The golden standard treatment for tracheal disorders is resection with primary anastomosis, where the damaged tissue is excised and the trachea is reconnected. This treatment can only repair up to 50% of the adult trachea and up to 30% of the pediatric trachea. Alternative treatment like patch or slide tracheoplasty, where the narrowed tissue is widened and slide together, is limited to repair only 30% of the trachea[9]–[11]. Patients with long segment tracheal disorders have no clinically feasible options. There is a strong clinical need for long-segment tracheal replacements beyond surgical limits, especially in children and emergency cases.

1.2 Tracheal Replacements Strategies

The ideal tracheal replacement mimics the structure and function of the trachea: a rigid hollow tube preventing airway collapse and epithelium-coated to prevent infection. The

replacement would mimic the extracellular matrix (ECM) of the trachea biochemically and biomechanically, while being porous to allow for ingrowth and vascularization. Airtight implantation of the patient-specific implant should be straightforward, with no host response to the biocompatible material and follow-up procedures required. Minimal preparation time with high replacement availability is desired with long-term growth considerations.

1.3 Tracheal Prostheses and Grafts

Tracheal replacements have utilized synthetic prostheses and non-viable biological tissues[12]–[14]. Solid prostheses kept the airway open but were often dislodged, caused infection, and formed granulation and scar tissue leading to restenosis or re-narrowing of the trachea [9]. Porous scaffolds such as meshes have been implanted with growth factors such as basic fibroblast growth factor (bFGF) and bone morphogenetic protein 2 (BMP-2) to recruit host cells to the implant site [15]–[20]. Despite good mechanical function, graft migration, host rejection and non-repopulation still led to infection problems, scaring, and restenosis. Harvesting autologous costal cartilage graft to patch the injured segment has proven effective for small tracheal defects[9]. The most glaring limitation is the lack of autologous donor sites, preventing long-segment replacement due to the shortage of accessible cartilage for tracheal repair. Xenotransplantation can offset organ donor shortage, but ethical concerns, fear of cross-species infection and host rejection have delayed clinical implementation [21].

Cell-free tracheal allotransplantation has been performed on compassionate grounds to provide the best quality of life for patients[22]. The most notable clinical example

involves non-decellularized tracheal allografts without epithelium and cultured *in situ* within immunosuppressed patients for 3 months for graft repopulation. The cellularized replacement then replaced the damaged trachea, a procedure which 5 patients have received [22], [23]. Results have been promising in terms of mechanical function and vascularization, but mediocre in terms of cartilage and epithelium repopulation as tissue necrosis was observed [24]. The potential benefits of allotransplantation are limited by donor supply and the need for immunosuppression [25]. Tissue-engineering methods seeding autologous cells on an appropriate scaffold obviate the need for immunosuppression, ultimately representing a viable tracheal replacement strategy.

1.4 Research Objectives

The goal of this research was to create a seamless cartilage cylinder for tracheal tissue engineering using scaffold-free techniques *in vitro*. While cartilage sheets have shown potential in tracheal tissue engineering, creating a seamless cartilage cylinder has not been explored using scaffold-free methods. The approach taken here seeded chondrocytes within tracheal moulds for roller bottle culture. Constructs were then rotated either manually or automatically to determine their effects on tissue growth. Optimal rotational speeds and growth factors were explored. Lastly, cell layering was explored to produce a cartilaginous tube for tracheal replacement.

2 Literature Review

2.1 Tracheal Anatomy and Physiology

The trachea (windpipe) is a hollow tubular organ that facilitates airflow from the larynx to the bronchi for respiration. There are 4 tissue layers comprising the tracheal walls: the mucosa, submucosa, cartilage, and adventitia (Figure 2.1). The mucosa is the most luminal layer of the trachea consisting of pseudostratified columnar epithelium embedded with ciliated, brush, basal, and goblet cells on a basement membrane. Goblet cells generate mucous which covers the cilia and traps foreign bodies before reaching the lungs for removal (mucociliary clearance). Beneath the mucosa is the submucosa, comprised of areolar tissue containing blood vessels and nervous tissue for vascularization and innervation of the other tracheal layers [26]. The submucosa is supported by 15-20 C-shaped hyaline cartilage rings which prevent airway collapse and are connected to each other by elastic connective tissue. The trachealis, a longitudinal smooth muscle, joins the ends of the cartilage rings and facilitates airflow by construction and dilation. The outermost tracheal layer is the adventitia comprised of areolar tissue that anchors the trachea to the surrounding tissues. A mature trachea is 10-13 cm in length and 1.5-2.5 cm in diameter, while an infant trachea is 4 cm in length and 0.36 cm in diameter [1], [27].

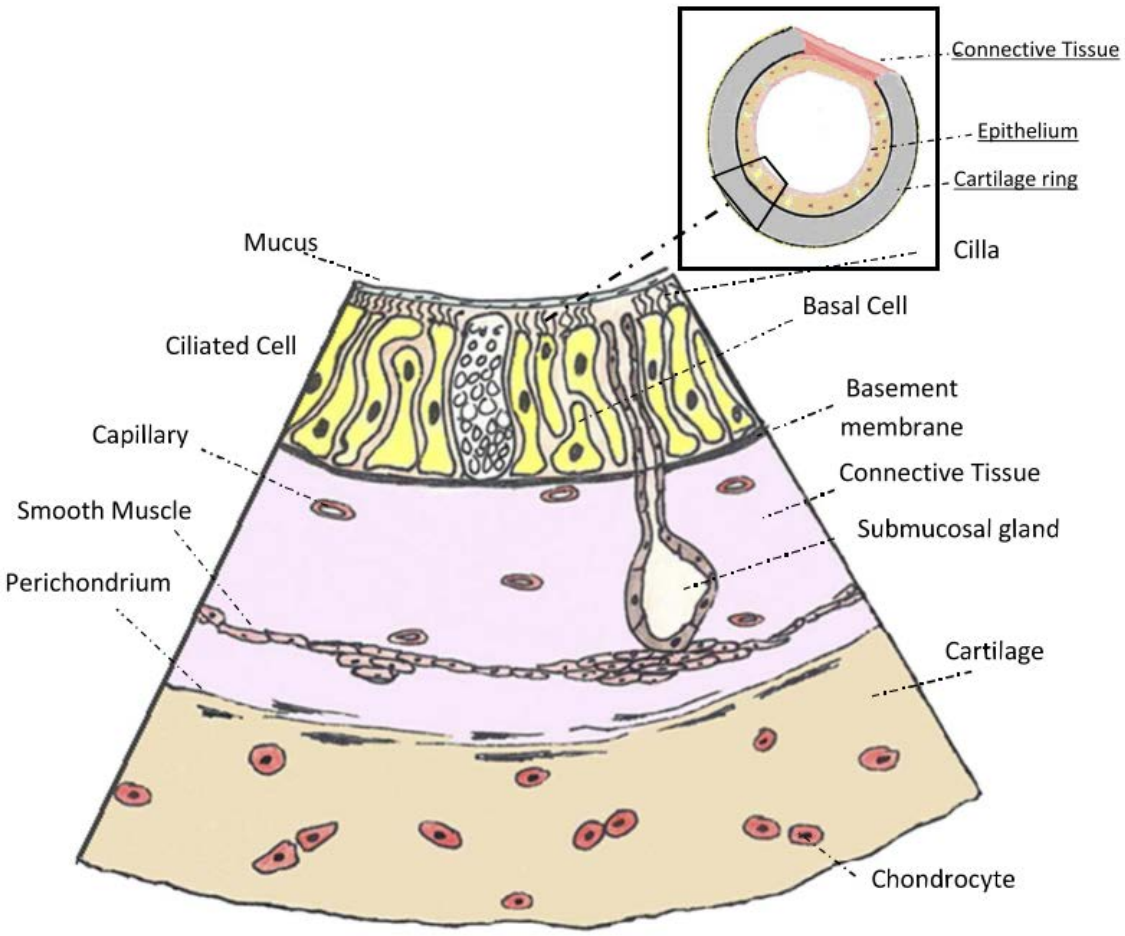

Figure 2.1: Diagram of the trachea and cross-section of the trachea[1]

2.1.1 Tissue Constituents

Chondrocytes are the only cells of cartilage, responsible for secreting the extracellular matrix (ECM) consisting mainly of collagen and proteoglycans. Cartilage is avascular, relying on diffusion to received nutrients and remove waste. Compared to other vascularized cells, cartilage suffers from relatively low proliferation rates and have a low cellular density [28]. The bands of fibrous tissue connecting the hyaline cartilage rings are called the annular ligaments of trachea and are comprised of fibroblasts. The

trachealis which joins the cartilage rings together is made of smooth, non-striated muscle cells which cause the tissue to contract, ultimately modulating size of the airway[26].

The pseudostratified columnar epithelium is actually a single layer of cells with varying nuclei position to give the appearance of cellular stratification[26]. The epithelium lines the tracheal lumen with a network of ciliated, basal, and secretory cells on a basement membrane. Goblet cells secrete mucous to trap particulates which works together with ciliated cells propel particulates for expulsion to prevent pathogens from reaching the lungs (mucociliary clearance). Basal cells line the basement membrane have the ability to differentiate to any cell type found in the epithelium, often migrating to injury sites for regeneration[26].

2.1.2 Extracellular Matrix (ECM)

2.1.2.1 Water

Water accounts for nearly 80% of the wet weight of cartilage, with 30% of this water filling the space between the collagen networks and 70% filling the ECM's pore space [29]. The interstitial fluid is comprised of water and dissolved ions such as sodium, calcium, chloride and potassium [29], to generates frictional resistance and water pressure allowing loading. Water flows throughout the cartilage to transport nutrients to chondrocytes as well as lubricate surfaces.

2.1.2.2 Collagen

Collagen comprises 60% of the dry weight of cartilage and is the most prevalent macromolecule. Specifically, type II collagen represents 90-95% of the ECM collagens [29]. Other collagen types such as collagen types V, VI, IX, X and XI help form and stabilize the type II collagen network. The collagen molecule is a three polypeptide chain of often of “glycine-proline-hydroxyproline”. Hydroxyproline stabilizes collagen by formation of hydrogen bonds and cross-links between collagen chains, resulting in ECM strong in tension[29].

2.1.2.3 Proteoglycans (PG)

Proteoglycan (PGs) represent the second largest macromolecule of the ECM in articular cartilage, accounting for 10-15% of its wet weight. PGs consist of a protein core with multiple polysaccharide glycosaminoglycan (GAG) chains attached. The largest and most abundant GAG is aggrecan, which possesses more than 100 chondroitin sulfate and keratin sulfate chains [29]. Aggrecan occupies the intrafibrillar space of cartilage and produces the osmotic property that hydrates or swells cartilage with water for compressional strength.

2.1.3 Tracheal Biomechanics

Despite both using hyaline cartilage, tracheal cartilage differs greatly from articular cartilage in its structure and function. Articular cartilage is thinly layered to withstand the compressive loads while tracheal cartilage uses thick circular rings to maintain airway

patency. Traditional cartilage biomechanical assessments include compressive, tensile, and shear testing, evaluations that not fully assess tracheal function. As a hollow tube under dynamic stresses, physiological-relevant loads must be considered in determining a trachea's resistance to collapse. One test places tracheal segments into custom-made chambers and increases the external pressure until collapse, using video to record the modes of failure [15]. Another test uses a peristaltic pumps to produce intraluminal pressure until failure, recorded with a micro-computed tomography scanner [30]. Trachea compression test are radially focused for its circular geometry [31]. Tracheal tensile testing uses conventional uniaxial methods, securing strips between the grips of a mechanical tester and straining the tissue until failure to determine stiffness (Figure 2.2) [32]. Having a standardized set of tracheal mechanical tests would regulate comparative assessments.

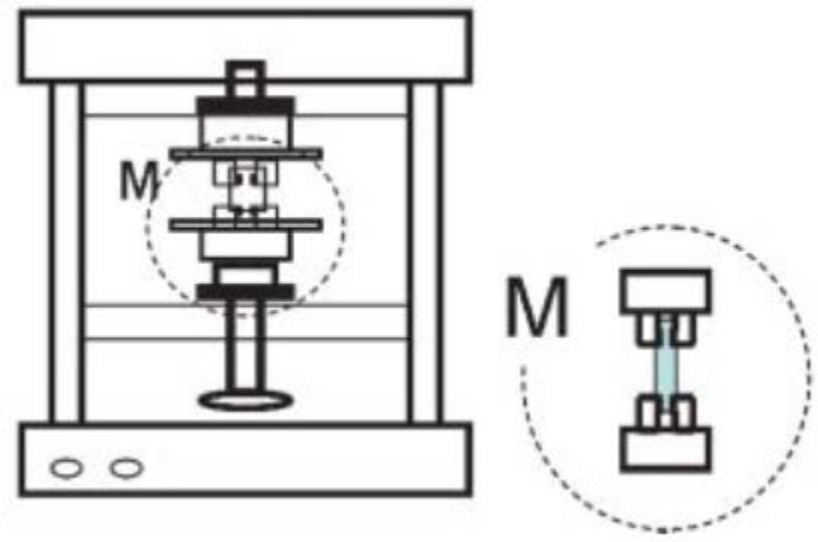

Figure 2.2: Tensile testing setup[32]

2.2 Tracheal Tissue Engineering

2.2.1 Scaffolds

2.2.1.1 Decellularized Scaffolds

Clinically, decellularized scaffolds are the most prominent tracheal replacement strategy, where cadaveric donor tissue is decellularized though a detergent-enzymatic method (DEM) to remove host cells and then reseeded with autologous cells. Using native tracheal tissue, these replacements have the desired biomechanical and biochemical properties without the risk of host rejection [33]. The first human tissue engineered tracheal replacement utilized a decellularized scaffold seeded with epithelial cells and mesenchymal stem-cell-derived chondrocytes in a 30-year-old female patient with bronchomalacia [34]. The scaffold was mechanically robust with no signs of host response and exhibited good revascularization and epithelialization[34]. At the 5-year follow-up, the trachea was patent and completely covered with functioning respiratory epithelium. Ciliary function and mucus clearance were fully observed, however, weak patency of the respiratory lumen required stenting [35]. The first pediatric tissue-engineered tracheal replacement utilized a decellularized scaffold to repair a damaged tracheal segment 7 cm long in a 10-year-old boy [36]. Autologous cells were seeded at implantation with granulocyte-colony stimulating factor (G-CSF) and transforming growth factor beta (TGF-b) as time was a limiting factor. At the 4 year follow-up, stenting was required once to clear mucus build up causing infection and stenosis [37].

There are a wide variety of DEMs, each offering various benefits and complications [30], [38]–[43]. Trace amounts of host cells could generate an immune response, thus a guideline of <50 ng DNA/mg tissue (dry weight) has been suggested [40]. To achieve

this level of antigen removal, the vigorous agents such as enzymes, detergents and physical forces are required which damage the ECM of the scaffold [40]. Immediate testing after decellularization usually shows minimal decrease in mechanical properties and ECM constituents [38], [43], [44]. Long-term testing reports reduced collagen and elastin content corresponding to decreased mechanical properties in decellularized tracheas [45]. Preparation time also varies from 1-45 days [34], [42], [46]; the latter being unsuitable for emergency tracheal replacement.

Clinical success has been achieved in compassionate cases, but further refinement is needed to get this procedure into clinical trials [33]. A review of nine adult and pediatric patients were reported no graft related mortalities 1-2 years post transplantation, however, graft collapse has persisted [47]. The biggest hindrance is the lack of donors, both in terms of supply and customization for a patient [48]. Optimized DEMs could re-establish xenotransplantation as a primary means of farming donor organs [25]. For pediatric cases, decellularized tracheal replacements are not viable long-term as the scaffold may not degrade with the rate of the child's growth.

2.2.1.2 Synthetic Scaffolds

Synthetic scaffolds can be fabricated from various materials and methods with high control over properties. This has resulted in two clinically successful synthetic tracheal replacements. A composite scaffold of Marlex mesh and collagen sponges patched smaller defects in the larynx and trachea in 4 patients [49]. At the 34-month follow-up, good epithelization was observed in all 4 patients; however, one patient exhibited an air leak. The first synthetic tracheal transplant occurred in 2011 on a 36-year-old male with

tracheal cancer too large to be resected [50]. A tailor-made nanocomposite polymer (POSS-PCU) was seeded with autologous bone marrow cells for 36 hours in a custom-made bioreactor and then implanted into the patent [50]. The POSS-PCU nanocomposite was chosen for its mechanical properties, biocompatibility, and low inflammatory response *in vivo* [51], [52]. Bacterial and fungal infection appeared 1 week post-operatively, after 5 months the patient was without symptoms having a patent, vascularized, and epithelialized airway [33].

Synthetic scaffolds present immense potential but must address long-term concerns. The high control over properties such as porosity and structure allow for patient-specific scaffold to be readily fabricated. Problems of contamination, stiffness, degradability, and inflammatory response still remain. The large variety of materials and methods requires further refinement for widespread clinical implementation. For pediatric use, a scaffold degrading with the rate of tissue formation would circumvent follow-up surgeries as the patient grows, however, degradation by-products and resulting mechanical losses must be considered. Recent cases of scientific misconduct by Paolo Macchiarini have greatly limited the clinical translation the POSS-PCU scaffold, as between 2011 and 2014, 9 cases of synthetic tracheal transplantation occurred, 7 of which have died [53].

2.2.2 Cell Sourcing

Cell sources can be a limiting factor in tissue engineering. For autologous cells, donor sites must be minimally invasive yet generate sufficient cell yields to repopulate the graft. Cellular proliferation must be considered with respect to preparatory time, as passaging cells to get the desired cell number may not be an option in emergency

cases. Cellularly sparse and non-vascularized tissue like cartilage has a low regenerative capacity and requires larger biopsy to generate the desired cell yield. Chondrocytes have also been known to dedifferentiate in monolayer with passaging [54]. Thus, primary autologous chondrocytes are often used from the trachea, nasal septum, knees, and ribs [55]. While procuring primary autologous chondrocytes may not be ideal, stem cells, which exhibit a high regenerative capacity and can differentiate into chondrocytes, are easier to access.

Mesenchymal stem cells (MSCs) have the ability to differentiate into various cell lineages making them attractive for tissue engineering. Stem cells sources include adipose tissue, bone marrow, endometrial tissue, synovium and blood [1]. The most assessable MSC sources are bone marrow and adipose stem cells acquired through needle aspiration. These cells have been researched extensively in cartilage regeneration [56]. Other researched stem cells include embryonic stem cells (ESCs) and induced pluripotent stem cells (iPSCs). ESCs exhibit unlimited self-renewal and pluripotency, potentially generating an unlimited supply of chondrocytes for regeneration [57], [58]. The potential of ESCs, however, are limited by ethical concerns in clinical translation. iPSCs addresses this concern by reprogrammed somatic cells, often dermal fibroblasts, for pluripotency [59]. As a non-invasive cell source with high regeneration and reprogrammable ability, iPSCs have immense potential in tracheal tissue engineering [60], [61]. iPSCs have problems adhering to their reprogrammed lineage and are prone to tumourgenicity [33], ultimately requiring further refinement for clinical implementation.

Epithelial cells also exhibit low regenerative capacity and often dedifferentiate past passage 4 [27], [62], a limiting factor for re-epithelization. Epithelial cells are often sourced from right main bronchus [63], [64] and passaged to generate the desired cell numbers. [65]. Epithelial cells are cultured in an air-liquid interface (ALI), where only the basal surface of the cells makes contact with media through a permeable membrane[66], [67]. Co-culture with fibroblasts, however, has shown increased epithelium expansion.

2.2.3 Scaffold-Free Tissue Engineering

Scaffold-free tissue engineering uses autologous cells to synthesize matrix without exogenous scaffolds. This leverages the customizability of synthetic scaffold methods with the biomimetics of decellurization without worry of a host response. In tracheal tissue engineering, cartilage cell sheets are grow, potentially layered, and rolled together to form a hollow cylinder [68]–[71]. These methods require a suture to hold the tissue together and foster tissue fusion. Another method fused cartilage rings together to form a cylinder not requiring sutures and exhibited increased axial mechanical strength; however, this may be the result of TGF-β1-containing gelatin microspheres acting as a scaffold. Scaffold-free tissue engineering has not created a seamless cartilage cylindrical for tracheal tissue engineering.

The trade-off for natural biocompatibility comes in preparation time. Synthetic scaffolds provide an “off-the-shelf” option for when time is a factor. Decellularized scaffolds require less preparation time, as the ECM is already established and cells need only infiltrate the scaffold. Scaffold-Free tissue engineering requires a large cell yield to build

and grow to the desired size, a process that would take months when hours are available.

2.3 Biochemical Signalling Molecules

Various growth factors have been used in tracheal tissue engineering, including erythropoietin [50], [72], basic fibroblast growth factor (bFGF) [19], [20], transforming growth factor beta (TGFβ) [73], vascular endothelial growth factor (VEGF) [74], and granulocyte colony-stimulating factor (G-CSF) [50], [72]. Synthetic scaffolds are often embedded with growth factors to enhance tissue growth *in vitro* to recruit host cells *in vivo* [19], [73], [75]–[78]. Growth factors can be directly administered to the defect site, either with or after implantation to promote engraftment [36], [50], [72]. The slow release of bFGF in native rat tracheal cartilage has promoted cellular growth and matrix production, with the resulting tissue being more resistant to collapse [15], [75], [79]. Growth factors relating to the TGF superfamily have traditionally enhanced cartilage matrix production. The combination of bone morphogenetic protein 2 (BMP-2) with insulin-like growth factor 1 (IGF-1) doubled the glycosaminoglycan (GAG) content and aggregate modulus or newly formed cartilage [80]. TGFβ has been shown to support chondrogenesis *in vitro* [48]. *In vivo* growth factor supplementation is usually directed towards neovascularization by incorporating factors that encourage angiogenesis such as erythropoietin, VEGF, and G-CSF [81], [82]. Overall, growth factors are imperative for recruiting stem or progenitor cells, promoting revascularization and innervation, and optimizing tissue structure/function. Despite the possible benefits, growth factors have the possibly for malignancy and dosage must be carefully monitored[24].

2.4 Bioreactors in Tracheal Tissue Engineering

Bioreactors aim to mimic the body's physical and mechanical stimuli to encourage tissue growth beyond static culture [53]. This is paramount in tissue engineering where constructs have high cellular densities requiring vigorous nutrient supply[83]. Dynamic bioreactors generate homogenous cell distribution, diffusion, and mechanical stimulation to encourage tissue growth[84]. For tracheal tissue engineering, the desired bioreactor would seed both chondrocytes and epithelial cells, generate rotation for homologous cell distribution, produce hydrodynamic stimulation, incorporate oxygenation, and encourage mass transfer under sterile conditions [85]. This must be done at a clinically relevant scale, specifically generating at least construct of 4 cm length, for long-segment tracheal replacement[86].

Tracheal tissue engineering in bioreactors initially focus on cartilage only, then combined epithelial cells onto tubular tissue. The perfusion seeding of chondrocytes demonstrated more homogenous cellular distribution and proliferation [87], and chondrocytes grown in a rotational bioreactor exhibited higher proliferation and ECM formation along the direction of flow[88]. These elements were implemented with epithelial cells in a rotating, double-chamber bioreactor for decellularized tracheas (Figure 2.3: Three-dimensional view of a rotating double-chamber bioreactor[86]Figure 2.3, Figure 2.4) [86]. This design cultured two different cell types on separate sides of decellularized scaffold, which is imperative for long-term organ replacement success as per clinical data [89]. Because of the different cell types, different culture medium was required for each tissue type. This bioreactor was used for the first successful airway

transplantation to re-seed the autologous cells onto the decellularized donor trachea [34]. Static seeding was replaced with dynamic perfusion seeding which further increased cellular counts and homogeneity of the decellularized scaffold[83].

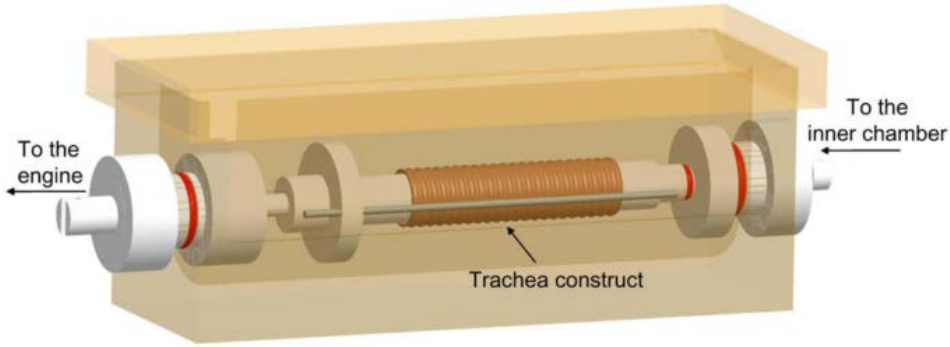

Figure 2.3: Three-dimensional view of a rotating double-chamber bioreactor[86]

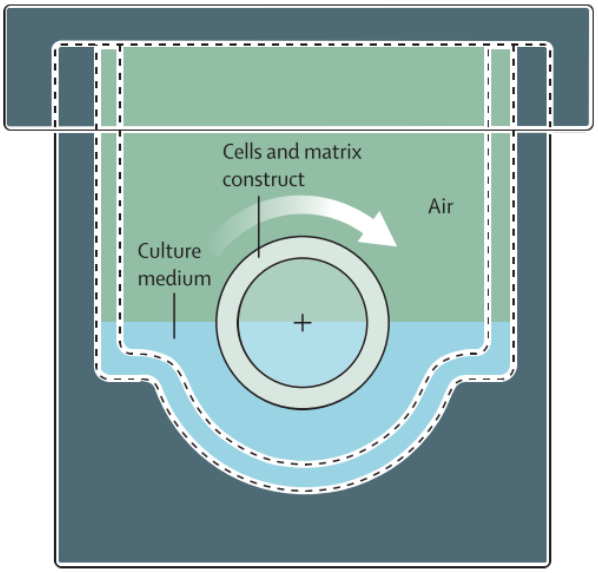

Figure 2.4: Lateral schematic of bioreactor[34]

Recent studies have used the body as an *in situ* bioreactor, leveraging the vasculature of the body for graft growth while decreasing related costs by lowering the risk of contamination and reducing processing time[72]. Implantation of chondrocytes-seeded tracheal constructs in mice generated tissue similar to mature hyaline cartilage after eight weeks [90]. Decellularized tracheal grafts implanted into mice were recellularized and exhibited well-organized cartilage with the presence of blood vessels [46]. Scale up to decellularized pig tracheas seeded *in vivo* alongside with cells and growth factors generated a mechanically suitable trachea with reparatory epithelium after 2 weeks and encouraged recruitment of progenitor cells [72]. The most notable clinical *in vivo* bioreactor example involved the successful allotransplantation of a non-decellularized tracheal graft in a patient's left forearm prior to implantation [22]. After 4 months *in situ*, respiratory epithelium was observed. After immunosuppression was suspended, the allograft was implanted to the trachea and which remained stable and functional after 2 years.

While both *in vitro* and *in vivo* bioreactors have their benefits, the most comprehensive solution would implement both strategies. First culturing chondrocytes and epithelium *in vitro* can allow for factors such as rotation, convention, and fluid shear to be controlled. Following this, the tissue can be implanted in situ to benefit from the vasculature of the body, and ultimately be transplanted to the defect site.

3 Materials and Methods

3.1 Bovine Articular Cartilage Harvest and Isolation

Bovine articular chondrocytes were isolated from calves (12 - 18 month old) or cows (18 - 24 month old) from Agram Meats (Georgetown, ON) on the day of slaughter. Cartilage slices were aseptically extracted from the metacarpal-phalangeal joint. The slices were then digested in 0.5% protease (w/v) (Sigma-Aldrich) in 20 mL of Ham's F12 media (HyClone, Logan, UT) buffered with 25 mM (Bioshop®, Burlington, ON, Canada), and incubated for 90 minutes (37°C, 95% relative humidity, 5% CO_2). The cartilages slices were then washed with Ham's F12, given 20 mL of 0.15% collagenase A (w/v) (Roche Diagnostics, Mannheim, Germany) in Ham's F12 media, and incubated for an additional 18 hours. The following day, the cartilage tissue digest was filtered through a size 200 mesh (Sigma-Aldrich) to remove undigested tissue and then centrifuged (700 RFC, 7 minutes). The resulting chondrocyte pellet was suspended in 20% FBS (v/v) in Ham's F12 media supplemented with 1% (v/v) antibiotic solution (100 U/mL penicillin, 100 mg/mL streptomycin, 0.25 mg/mL amphotericin B) (Sigma-Aldrich, Oakville, ON). Chondrocytes were suspended at a density of 1×10^6 cells/mL with cell viability was assessed using the Trypan Blue (Sigma-Aldrich) dye exclusion assay.

3.2 Creation of Trachea Moulds

3.2.1 Polypropylene Tube Preparation

Polypropylene (PP) tubing (ID 12.700 mm, OD 15.875 mm) (Cole-Parmer, Montreal, QC) was cut with a single-edge blade into 30 mm or 60 mm length segments to represent the trachea. The PP tracheal moulds were sterilized in 70% ethanol for 1 hour

and then autoclaved. Following sterilization, the PP tube segments were plasma-treated (Harrick Plasma, PDC-32G, NY) to enhance chondrocyte adhesion by making the PP tubes more hydrophilic. The sterilized PP segments were sealed into the chamber of the plasma machine under vacuum, and segments were plasma treated with oxygen gas for 2 minutes. Following plasma treatment, the PP tube segments were extracted from the machine's chamber into sterile conical tubes prior to use.

3.2.2 Static Culture Trachea Construct Preparation

For static culture, 60 mm segments were pre-scored with a tube-cutter into 15 mm segments, allowing for easier sectioning into 15 mm segments to fit inside the wells of the 24-well tissue culture plate after seeding. These segments were also marked at the quarter radial mark to serve as indicators when manually rotating the PP tubes during static culture.

3.2.3 Roller Tracheal Construct Preparation

A hole was punched in the centre of the circular face of end caps (I.D. 12.7 mm) (Stockcap, Arnold, MO) using a 4 mm biopsy punch (Miltex, Oakville, ON). This hole served as an attachment point for the luer barb fittings (Cole-Parmer) which were sealed with Buna-N O-rings (I.D. 1.6 mm, McMaster-Carr) at the interface. The Buna-N O-rings and luer barb fittings were sterilized in 70% ethanol for 1 hour, and then autoclaved. The augmented end caps were sterilized in 70% ethanol overnight in a biosafety cabinet as they could not withstand autoclave sterilization. Following

sterilization, the plasma treated PP tube segments, modified end caps, O-rings, and luer barb fittings were brought into the biosafety cabinet. The O-rings were placed onto the barbs of the luer fittings and secured to the end cap's attachment point (Figure 3.1). Following this, the luer barb-sealed end caps were placed onto both ends of the plasma-treated PP tube segments, and the resulting roller tracheal constructs were prepared for seeding.

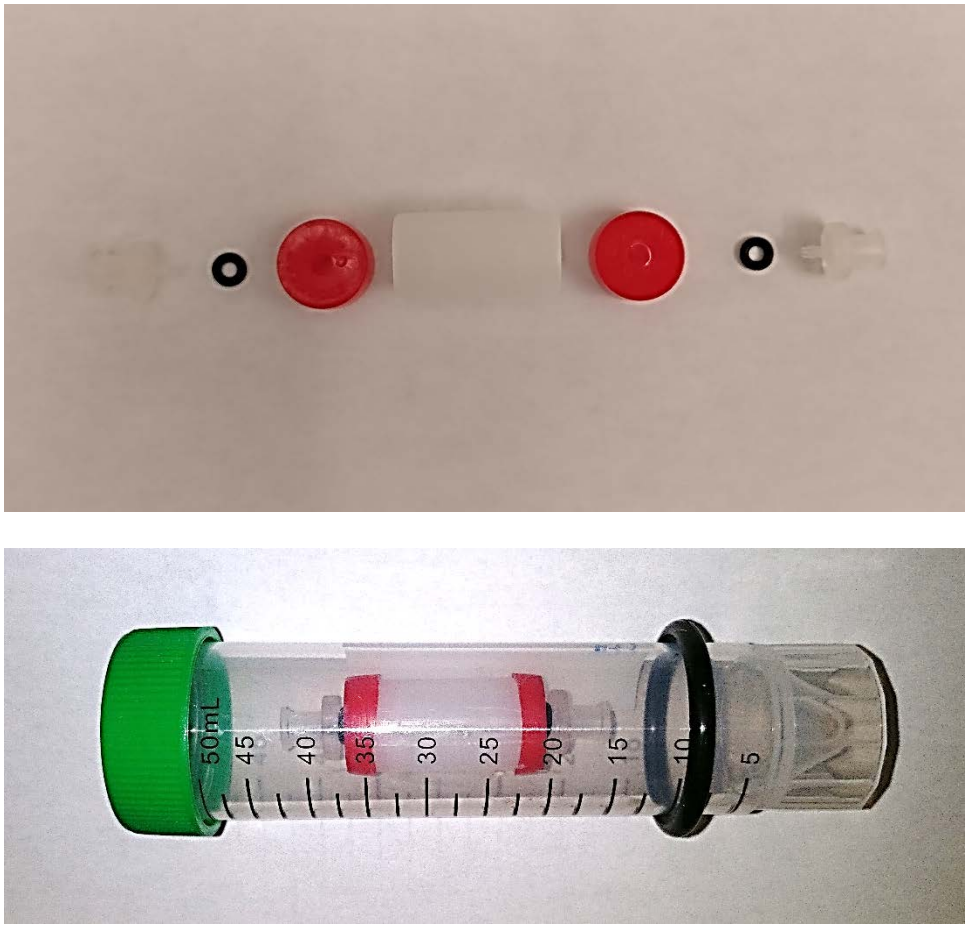

Figure 3.1: Assembly of Roller Tracheal Constructs within BioReaction Tube

3.3 Cell Seeding of Tracheal Moulds

The prepared bovine articular chondrocyte suspension ($1x10^6$ cells/mL) was seeded into the roller tracheal constructs through the luer fitting using a syringe. Chondrocytes were seeded by volume of the roller tracheal construct ($3x10^5$ cells/mm^3). The roller tracheal constructs were then returned to their respective Bio-Reaction tubes and onto the incubated bottle roller (Thermo Fisher Scientific) for 24 hours while rotating at 0.5 RPM.

3.4 Chondrocyte Adherence and Recovery

Chondrocyte were seeded onto the plasma-treated polypropylene (PP) tubes at various inoculation densities. Chondrocyte adherence was determined after 24 hour of seeding in the incubator on the bottle roller (0.5 RPM) using the Trypan Blue (Sigma-Aldrich) dye exclusion assay [91]. Adherent chondrocytes were trypsinized (0.05% trypsin, Life Technologies) from the chondrocyte-seeded PP tubes for 5 minutes (0.5 RPM, 37°C) and then counted. Non-adherence cells were determined by evaluating the effluent media.

3.5 Cell Culture

Tracheal constructs were cultured under static or dynamic conditions. Both static and roller culture were seeded similarly but differed in culture. All samples were fed every 2-3 days with 20% FBS (v/v) in Ham's F12 media, supplemented with 1% (v/v) antibiotics and 0.2% L-ascorbic acid (Sigma-Aldrich) (v/v). All cultures were maintained for a period of 4 weeks.

3.5.1 Static Culture

Following cell seeding, the tracheal constructs were brought back into the biosafety cabinet, the seeding media was aspirated, and the luer barb-sealed end caps were removed from the chondrocyte-seeded PP tubes. The PP tubes were cut along the premade grooves using a scalpel into 15 mm segments and placed into a 24-well tissue culture plate. The segments were fed 5 mL of their designated media, either: 1) no growth factor or 2) TGFβ1 (0.1 nM) (CM-TGF; PeproTech Inc., Rocky Hill, NJ, USA) supplemented media. Upon feeding, each segment was manually turned either a ½ rotation, ¼ rotation, or no rotation at each feed until the end of the 4-week culture period.

3.5.2 Roller Culture

After cell seeding, the roller tracheal constructs were brought back into the biosafety cabinet. The seeding media was aspirated and the luer barb-sealed end caps were removed from the chondrocyte-seeded PP tubes (30 mm length). The PP tubes were returned to their respective Bio-Reaction tubes and fed 15 mL of media, the maximal media level preventing the seeded PP tubes from floating during culture (Figure 3.2). Media was carefully exchanged to not disturb the tissue on the lumen of the roller trachea constructs, and Bio-Reaction tubes were replaced halfway through the culture period to maintain the filter's integrity.

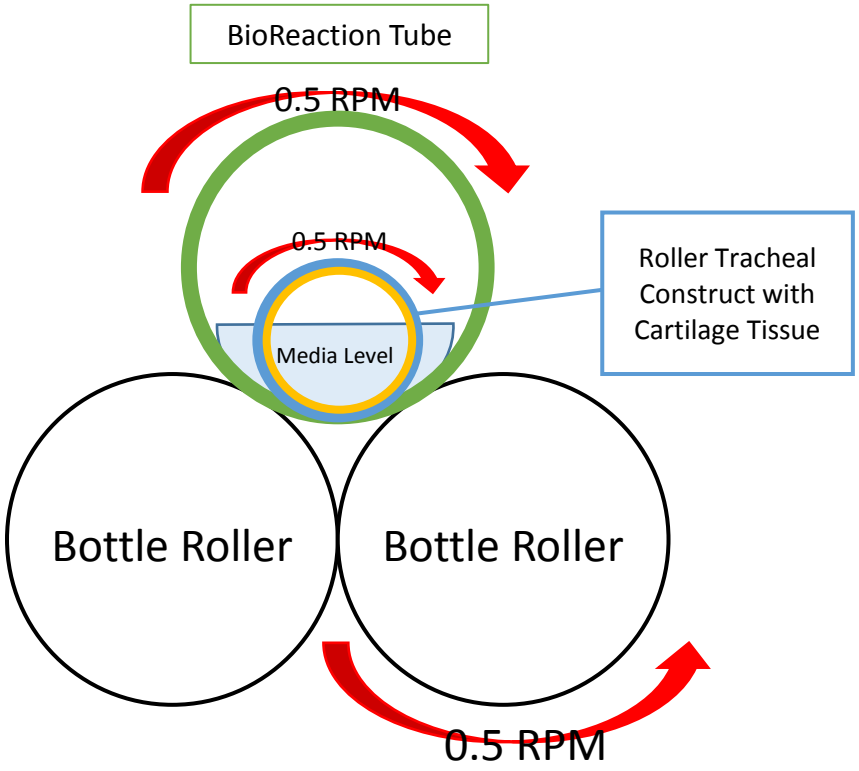

Figure 3.2: Experimental Set up for Roller Bottle Culture

3.5.2.1 Effect of Rotation Speed

The rotational speed of the constructs was varied to determine its effect on tissue growth. The bottle roller had a minimum rotational speed of 0.5 RPM, thus the diameter of the Bio-Reaction tubes was increased using plastic fittings to decrease the rotational speed of the constructs. Ultimately, the diameter-enlarged Bio-Reaction tubes spun at 0.1 RPM simultaneously with the Bio-Reaction tubes without fittings spun at 0.5 RPM on the same bottle roller unit until the end of the culture period.

3.5.2.2 Growth Factor Supplementation

Once the optimal rotational speed of the constructs was determined, growth factor supplementation was explored. All samples were cultured at a rotation speed of 0.1 RPM following cell seeding, and fed either 1) media without growth factors or 2) standard media supplemented by 10 nM IGF-1 (Peprotech, Rocky Hill, NJ, USA) until the end of the culture period.

3.5.2.3 Effect of Cell Layering

Cell layering was tested to determine its effect on tissue growth. When the isolated bovine articular chondrocytes (P0 cells) were seeded into the roller tracheal constructs, culture flasks were also seeded for expansion. These P0 cells were plated at a density of $6x10^3$ cells/cm^2 in 10% FBS (v/v) in Ham's F12 media supplemented with 1% (v/v) antibiotics. After seeding, the roller tracheal constructs were cultured at 0.1 RPM and fed either: 1) media without growth factors or 2) media supplemented by 10 nM IGF-1 (Peprotech, Rocky Hill, NJ, USA). Upon confluence, culture flasks were trypsinized

(0.05% trypsin (Life Technologies)), washed and counted. The resulting P1 cells were seeded on top the P0 cells of the roller tracheal constructs at a density of $3.3x10^7$ cells/mm^3. The P1 cells were also plated into culture flasks for expansion. When the P1 cells reached confluence, the layering process was repeated, with the resulting P2 cells seeded on top of the P1 and P0 cells. Roller tracheal constructs were fed their respective media and cultured at 0.1 RPM until the end of the culture period.

3.6 Assessment of Tissue Thickness & Mechanical Properties

3.6.1 Tissue Thickness Measurements

The thickness of the cultured tissues were determined using the needle probe method [92]. Harvested tissue biopsies were placed on a flat stainless steel stage, and a 25Ga needle (Becton, Dickinson and Company, Franklin Lakes, NJ, USA) was secured to a 1-kg (9.81-N) load cell of the Mach-1™ mechanical tester (Biomomentum, Laval, GC). The load cell and needle travelled towards the mounted tissue at 5 µm/s, and the Mach-1 Motion data acquisition software (Biosyntech) recorded the displacement of the needle and the resulting compressive forces at 10 Hz. Using a plot of the resistive compressive force as a function of needle displacement (Figure 3.3), the initial tissue contact and complete tissue penetration were characterized by inflections in the plot. Prior to tissue contact, the forces measured showed little change, however, upon tissue contact, the forces observed increased prominently. These forces gradually increased until tissue penetration and stage contact, upon which the forces measured spiked. The positional difference between these tissue contact and tissue penetration determined

tissue thickness. Tissue thickness was evaluated at two different locations at room temperature for each sample and averaged.

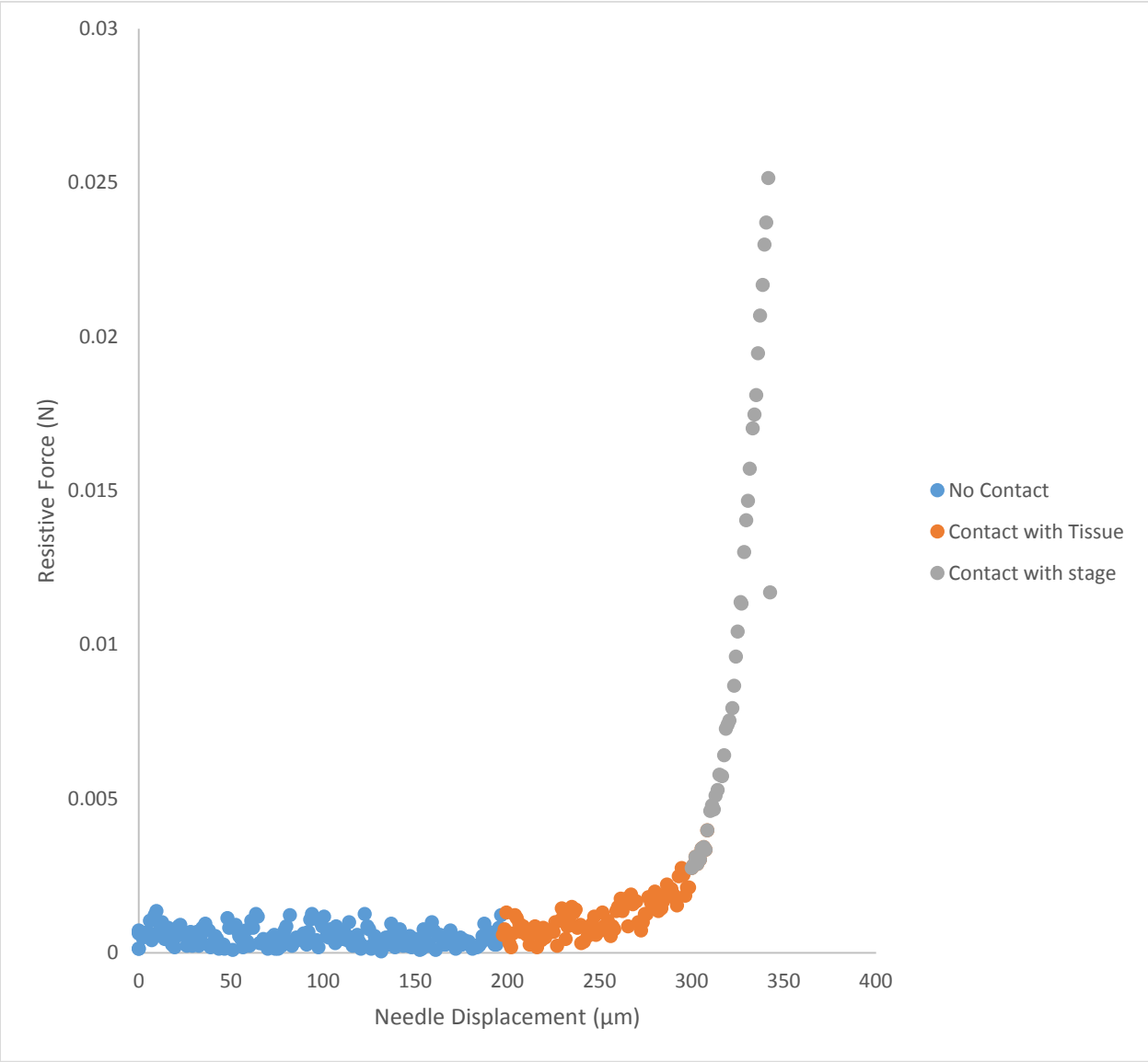

Figure 3.3: Resistive force as a function of needle displacement

3.6.2 Tensile Mechanical Testing

Both circumferential and longitudinal strips were excised from the harvested cylindrical cartilaginous tissue for tensile testing. The strips (100 µm thick, 3 mm wide, 10 mm long) were measured in uniaxial tension using the Mach-1™ micromechanical tester (37°C). To secure the strips to the grips of the mechanical tester, windows frames were cut out of adhesive name tags (Avery, Canada) with an inner square (7 mm x 7 mm). The cartilaginous tissue strips were secured between these “adhesive windows” and mounted to the mechanical tester’s grips. Samples were strained at 1% strain s^{-1} until failure, with the load and displacement sampled at 10 Hz. Tensile stress was calculated as the measured tensile force (load cell) normalized to the cross-sectional area (thickness x width) of the mounted strips. The applied strain was measured as the deformation normalized to the gauge length of the strip (7 mm). The stress-strain curve was plotted, with the linear (elastic) region identified to calculate the modulus by linear regression (Figure 3.4).

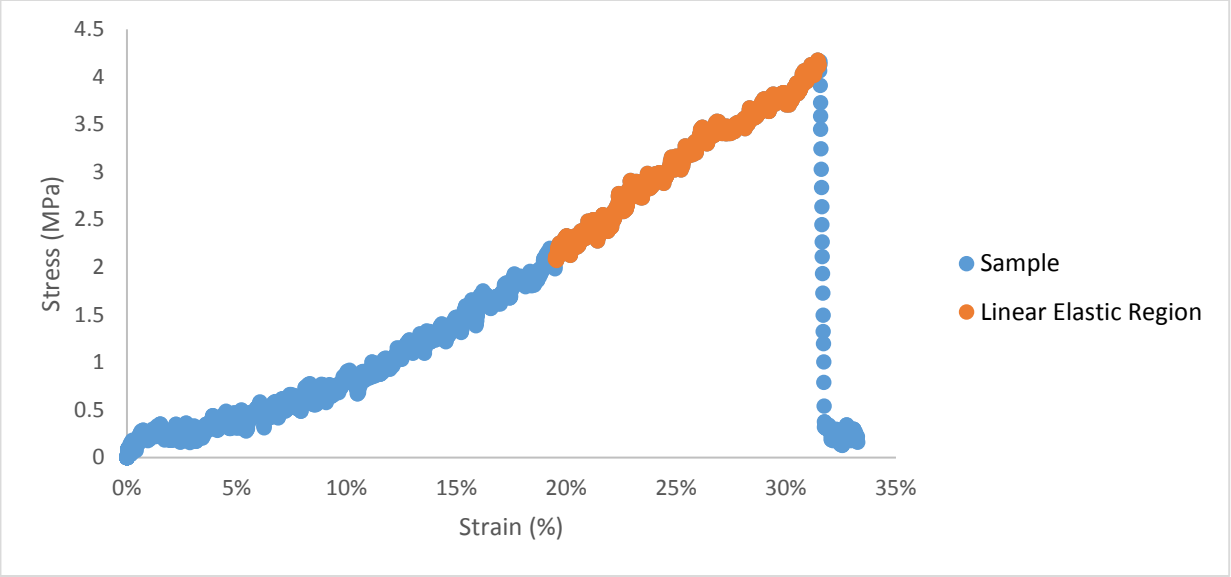

Figure 3.4: Stress-strain curve of cartilaginous tissue strip

3.7 Biochemical quantification of harvested constructs

3.7.1 Tissue Harvest and Wet/Dry Weight Measurements

Cartilaginous tissues were harvested from the PP roller tracheal constructs using a spatula and washed with PBS. Sections of the tissue were designated for biochemistry, histology, and mechanical testing. The wet and dry weights of the samples for biochemistry were determined to quantify the moisture content of the samples and to normalize biochemical assay results. The wet weights of the tissues were determined by recording the total mass (Mettler Toledo ME104E) of the tissue-containing micro-centrifuge tubes and subtracting the pre-determined mass of the micro-centrifuge tubes. The dry weight was determined after overnight lyophilisation under vacuum (-45°C) in the same fashion.

3.7.2 Tissue Digestion

Cartilaginous samples were digested to determine the mass of their biochemical constituents. Samples were digested in papain (static: 40 µg/mL, roller culture: 80 µg/mL) (Sigma-Aldrich) for 72 hours (65°C). The papain digest was then aliquoted and stored for further analysis (-20°C).

3.7.3 DNA, Glycosaminoglycan and Hydroxyproline Quantification

The accumulated DNA, glycosaminoglycan (GAG) and hydroxyproline content of the cartilaginous samples were determined using biochemical assays from the papain digest. All assays were performed in 96-well plates (VWR International, Mississauga, ON), with all standards and samples measured in triplicate. Assay results were normalized to DNA content and dry weight.

DNA content was characterized using Hoechst 33258 dye (Sigma-Aldrich)[93]. Papain digest was diluted with PBS (pH 7.4) and standard curves were generated using calf thymus DNA (Sigma-Aldrich). The diluted digest and prepared standards were added to 96-well fluorescence plates, and then mixed with dye solution. The fluorescence was measured at excitation (350 nm) and emission (450 nm), and the standard curves characterized the fluorescence recorded to the digest's DNA content.

GAG content was characterized using 1,9-dimethylmethylene blue (DMMB) (Sigma-Aldrich) dye to quantify sulphated glycosaminoglycans[94], [95]. Papain digest was diluted with 1% (w/v) bovine serum albumin (Sigma-Aldrich) in PBS (pH 7.4), with

standard curves generated using bovine cartilage chondroitin sulphate A (Sigma-Aldrich). The diluted digest and standards were added to 96-well plates, and then mixed with DMMB dye solution. The absorbance was measured (525 nm), and the standard curves characterized the absorbance recorded to the digest's GAG content.

Hydroxyproline content was measured though chloramine-T/Ehrlich's reagent [96], [97]. Papain digest was hydrolyzed in 6 N HCl (18 hours, 110°C), neutralized with 5.7 N NaOH, and then diluted with distilled water. Standard curves were generated using L-hydroxyproline (Sigma-Aldrich). The diluted hydrolysate and standards were added to the standard 96-well plates and then mixed with chloramine-T (Sigma-Aldrich) and Ehrlich's reagent (Sigma-Aldrich). Absorbance was measured at 560 nm, and the standard curve correlated the absorbance recorded to hydroxyproline content.

3.8 Histological Evaluation

Histological evaluation was conducted to visualize the cartilaginous tissue. Harvested samples were fixed in 4% paraformaldehyde dissolved in 0.1 M PBS overnight (4°C). Samples were then washed in PBS, stored in 70% ethanol (4°C), dehydrated in graded ethanol solutions, and paraffin embedded for sectioning. Sections (5 µm thick) mounted on Superfrost Slides (Fisher Scientific, Mississauga) and dried for 24 hours (37°C) prior to staining.

To identify proteoglycans, sections were stained with safranin O counter-stained with fast green, where cartilage stained orange/red and nuclei stained black. Briefly, the tissue sections were deparaffinised and rehydrated in water, stained with Weigert's iron haematoxylin for 10 minutes, and rinsed with tap water for 10 minutes. Then sections

were then counter-stained with 0.05% fast green solution for 5 minutes, and after a 15-second 1% acetic acid wash, the slides were stained with 0.05% Safranin O for 5 minutes. Lastly, samples were dehydrated in graded alcohol solutions, cleared in xylene and mounted using Permount resinous media (Fischer Scientific, Ottawa, ON, Canada). To visualize collagen within the tissue, sections were stained with Sirius red, where collagen stained red on a pale yellow background with black nuclei. Briefly, the tissue sections were deparaffinised and rehydrated in water, stained with Weigert's iron haematoxylin for 8 minutes, and rinsed with tap water for 10 minutes. Then sections were then stained with pico-sirius red for one hour, and after 2 changes in acidified water, vigorously shook to remove water. Lastly, samples were dehydrated in graded alcohol solutions, cleared in xylene and mounted using Permount™ resinous media (Fischer Scientific, Ottawa, ON, Canada). All sections were examined by light microscopy using Nikon Upright E800 Microscope.

3.9 Statistical Analysis

All numerical results are expressed as the mean ± SEM. For the effect of manual rotation experiments, data were compared between experimental groups using a one-way ANOVA, and statistical significance was determined using Tukey's multiple comparison's test with a single pooled variance (Graphpad, Prism, CA, USA). In the effect of rotational speed, growth factor supplementation, and layering experiments, data from each experimental group were compared using parametric, unpaired t-test with Welch's correction (Graphpad, Prism, CA, USA). Significant differences in all

experiments were associated with p values of less than 0.05, and trends were associated with p values between 0.05 and 0.1.

4 Results

4.1 Chondrocyte Adherence

Primary bovine chondrocytes were seeded onto the plasma-treated polypropylene tubes at various inoculation densities, ranging from 2.3×10^5 cells/cm^3 to 4.6×10^5 cells/cm^3. The seeded constructs were then incubated for 24 hours on the bottle roller (at a rotational speed of 0.5 RPM). After this seeding period, chondrocyte adherence and viability was determined using the Trypan Blue (Sigma-Aldrich) dye exclusion assay (Table 1). As the inoculation density increased, the percentage of adherent seeded cells decreased, but the number of live adherent cells to the tube plateaued at, and beyond the inoculation densities of 3.3×10^5 cells/cm^3. Since an increase in cell density could not increase adherence cell density at this point, an inoculation density of 3.3×10^5 cells/cm^3 was used for all subsequent experiments.

Table 1: Chondrocyte attachment to plasma-treated polypropylene constructs

Inoculation Density (cells/cm^3)	$2.3\text{x}10^5$	$3.3\text{x}10^5$	$4.6\text{x}10^5$
Total Live Cells on Tube (cells/cm^3 x 10^5)	1.02 ± 0.46	1.19 ± 0.52	1.13 ± 0.65
As a % of seeded cells	71%	59%	52%
Cell Attachment Density (cells/cm^2 ×10^4)	4.2 ± 0.12	6.17 ± 0.17	6.11 ± 0.20

Data presented as mean ± SEM (n=3-6).

4.2 Effect of Manual Rotation

Roller tracheal constructs were manually rotated by set amounts (½ of a turn, ¼ of a turn, or no turn) at each media exchange (48-72 hours) to optimise tissue growth. At the

end of the 4-week static culture period, samples were evaluated biochemically. Upon harvest, the samples rotated either ½ or ¼ of a rotation at each media exchange always exhibited full coverage of the roller tracheal construct. However, the samples not rotated at each media exchange were often void of tissue at the top of the roller tracheal construct's tube (data not shown).

4.2.1 Biochemical Evaluation

At the end of the culture period, samples were assayed for DNA, glycosaminoglycan, and hydroxyproline contents, all normalized to construct dry weight. Glycosaminoglycan and hydroxyproline content were also normalized to DNA content. The effect of manual rotation did not significantly affect DNA content ($p=0.85$) (Figure 4.1). Glycosaminoglycan content was not significantly affected by manual rotation, either when normalized to dry weight or DNA content ($p=0.40$ and $p=0.32$, respectively) (Figure 4.2). Hydroxyproline content was also not significantly affect by manual rotation, either when normalized to dry weight or DNA content ($p=0.40$ and $p=0.19$, respectively) (Figure 4.3). Overall, manual rotation did not have a significant effect on tissue growth biochemically, but was necessary to ensure full coverage of the roller tracheal constructs.

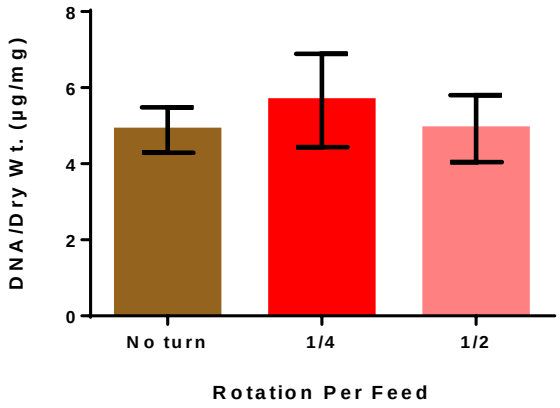

Figure 4.1: The effect of manual rotation on DNA content, normalized to dry weight

Data presented as mean ± SEM, n=3-9 samples per group.

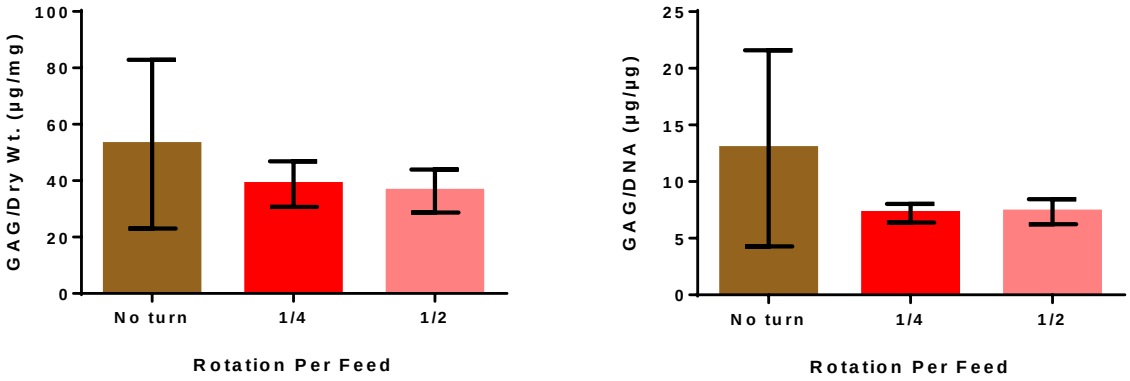

Figure 4.2: The effect of manual rotation on glycosaminoglycan content, normalized to dry weight and DNA content

Data presented as mean ± SEM, n=3-9 samples per group.

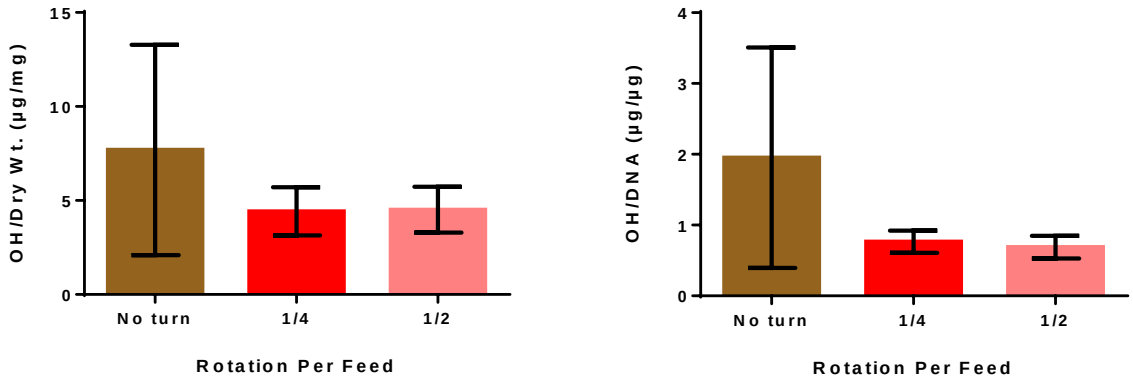

Figure 4.3: The effect of manual rotation on hydroxyproline content, normalized to dry weight and DNA content

Data presented as mean ± SEM, n=3-9 samples per group.

4.3 Effect of Rotational Speed

As manual rotation did not have a significant effect on tissue growth, the effect of automatic rotation on tissue growth was investigated. A bottle roller was used to continuously rotate the roller tracheal constructs at either slow (0.1 RPM) or fast (0.5 RPM) rotational speeds, with samples dynamically cultured under these conditions for a period of 4 weeks. At the end of the culture period, samples were harvested and analyzed biochemically and histologically. Upon harvest, all samples exhibited full coverage of the roller tracheal construct with apparent homogenous tissue distribution.

4.3.1 Biochemical Evaluation

At the end of the culture period, samples were assayed for DNA, glycosaminoglycan and hydroxyproline content, with the results normalized to dry weight. Glycosaminoglycan and hydroxyproline content were also normalized to DNA content. Dynamic rotation culture at the slower rotational speeds (0.1 RPM) did not significantly affect DNA content ($p=0.85$) (Figure 4.4). However, slower rotational speed did significantly increase GAG content, either when normalized to dry weight or DNA content ($p<0.05$, $p=0.07$, respectively) (Figure 4.5). Faster rotational speeds appeared to have drastically hindered glycosaminoglycan secretion. Hydroxyproline content, however, was not significantly affected by faster rotational speed either when normalized to dry weight or DNA content ($p= 0.53$ and $p=0.62$, respectively) (Figure 4.6). Overall, higher rotational speeds did not significantly affect DNA or hydroxyproline content, but had a significantly increased glycosaminoglycan synthesis. Because of the increased tissue accumulation observed at slow (0.1 RPM) rotational speed, all subsequent experiments were cultured at 0.1 RPM.

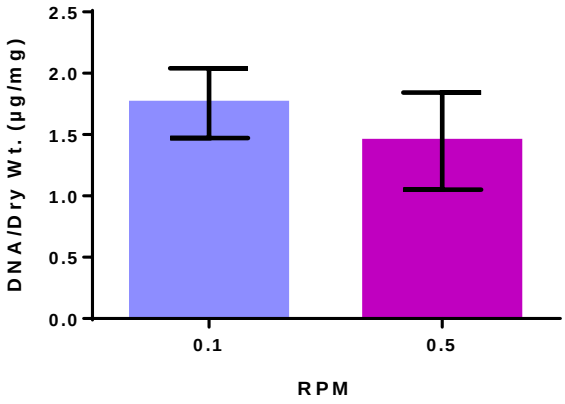

Figure 4.4: The effect of rotational speed on DNA content

Data presented as mean ± SEM (n=3-8 samples per group).

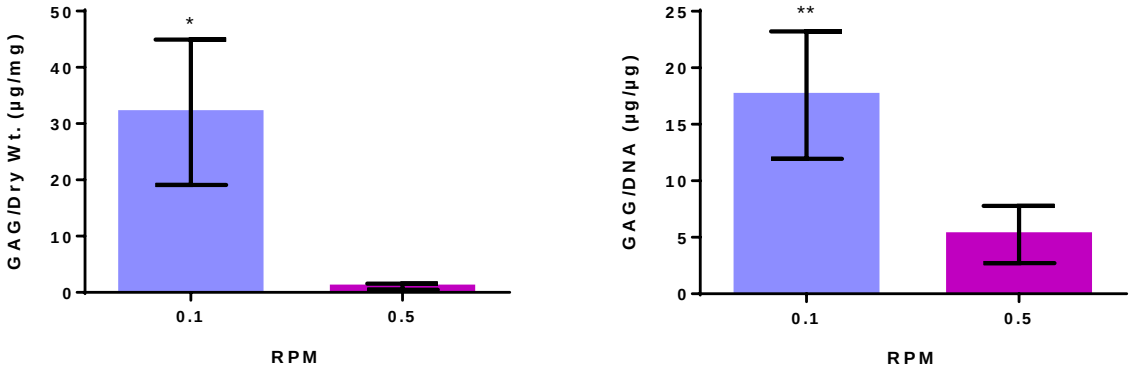

Figure 4.5: The effect of rotational speed on glycosaminoglycan content

Data presented as mean ± SEM (n=3-8 samples per group). *significantly different ($p<0.05$), ** trend ($p=0.07$).

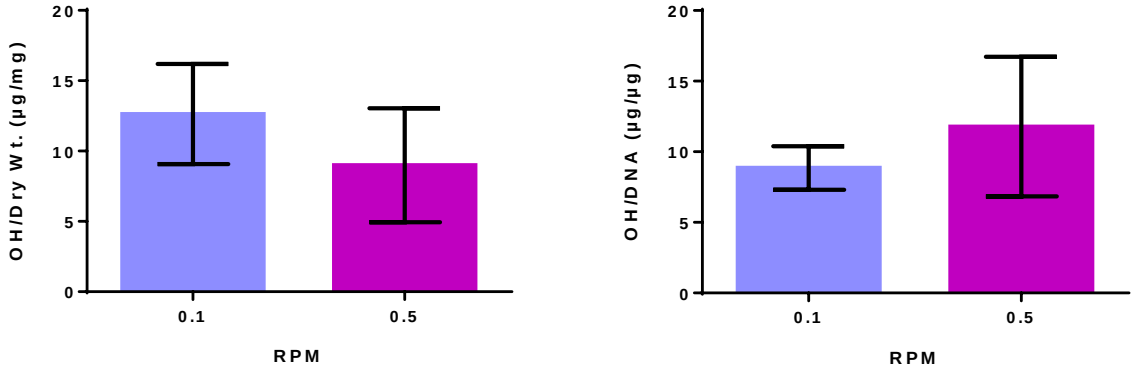

Figure 4.6: The effect of rotational speed on hydroxyproline content

Data presented as mean ± SEM (n=3-8 samples per group).

4.3.2 Histological Evaluation

At the end of the culture period, samples were fixed, sectioned, and stained with safranin O and sirius red to visualise glycosaminoglycan content and collagen content, respectively (Figure 4.7). Both the samples cultured at 0.1 and 0.5 RPM appear to have the same cellular density, supported by the similar results observed in DNA content when normalized to dry weight. Morphologically, chondrocytes appeared round in shape and were randomly dispersed throughout the tissue matrix in lacunae for both samples. Minimal glycosaminoglycan staining was observed for samples cultured at 0.5 RPM in the safranin O stains, however, diffuse positive glycosaminoglycan staining was observed for samples cultured at 0.1 RPM. The results of the safranin O staining correspond to decrease in glycosaminoglycan content observed biochemically in samples cultured at 0.5 RPM compared to those cultured at 0.1 RPM. This evidence strongly suggests that the higher rotational speed significantly negatively affected

glycosaminoglycan synthesis. The intensity of the sirius red staining was greater for samples cultured at the slower rotational speed, which corresponds to the increased hydroxyproline content observed biochemically when normalized to dry weight for samples rotated at 0.1 RPM. The thickness of the samples cultured at the slower rotational speed was at least twice that of the samples cultured at 0.5 RPM. Overall, the slower rotational speed produced thicker, glycosaminoglycan-rich tissue with increased collagen content observed biochemically and histologically.

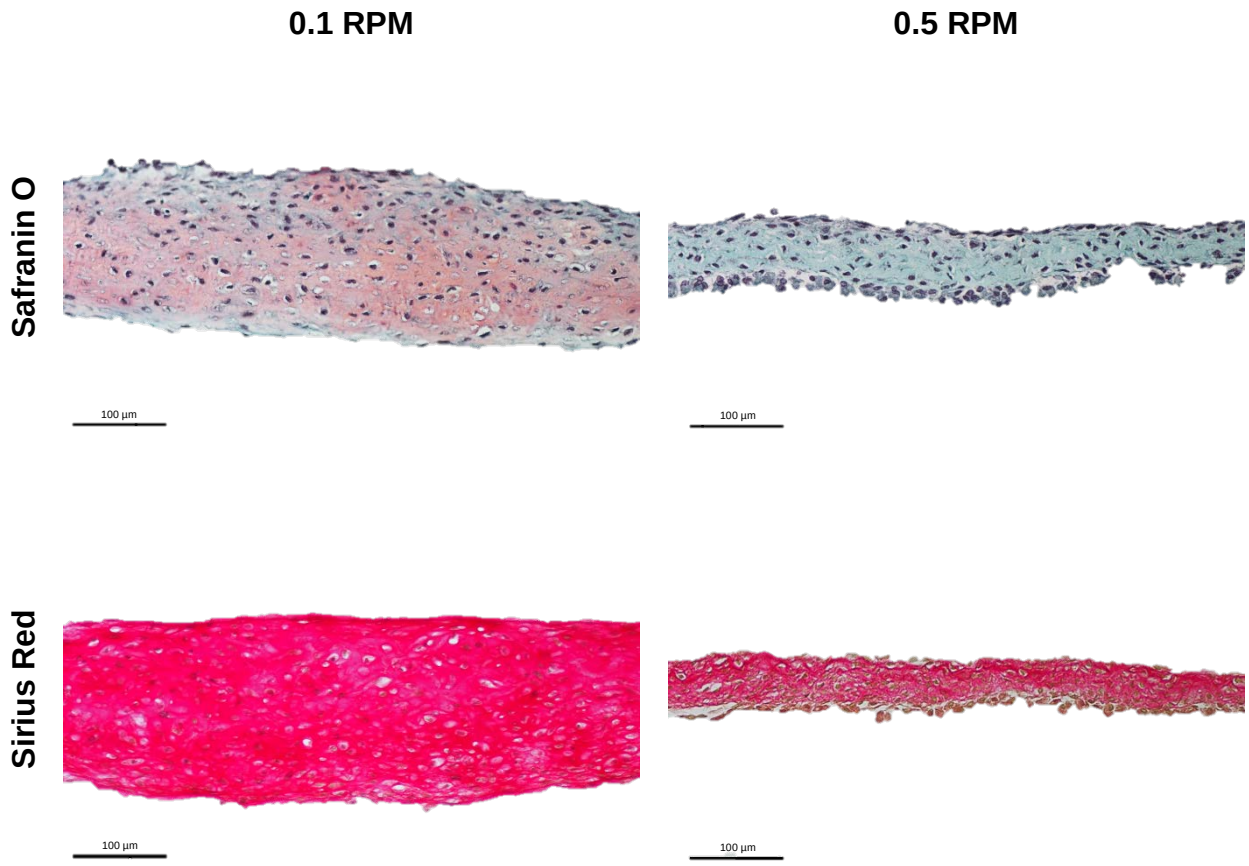

Figure 4.7: Safranin O and Sirius Red staining of cartilaginous tissue after culture at 0.1 and 0.5 RPM

4.4 Effect of Growth Factor Supplementation

As dynamic culture was optimized at a rotational speed of 0.1 RPM, the effect of growth factor supplementation on tissue growth was investigated. Roller tracheal constructs were cultured at 0.1 RPM either with or 10 nM insulin-like growth factor 1 (IGF-1) supplementation. At the end of the 4-week culture period, samples were harvested and analyzed biochemically, histologically, and for changes in physical properties. All harvested samples exhibited full coverage of the roller tracheal construct.

4.4.1 Biochemical Evaluation

At the end of the culture period, samples were assayed for DNA, glycosaminoglycan and hydroxyproline content, with the results normalized to dry weight. Glycosaminoglycan and hydroxyproline content were also normalized to DNA content. IGF-1 supplementation did not have a significant effect on DNA content ($p=0.18$) (Figure 4.8). However, while IGF-1 did not have a significant effect on glycosaminoglycan content when normalized to dry weight ($p=0.19$), a significant increase in glycosaminoglycan content was observed when normalized to DNA content ($p<0.01$) (Figure 4.9). Samples supplemented with IGF-1 also exhibited an increase in hydroxyproline content when normalized to dry weight ($p=0.10$). However, this trend was lost when hydroxyproline content was normalized to DNA content ($p=0.33$) (Figure 4.10).

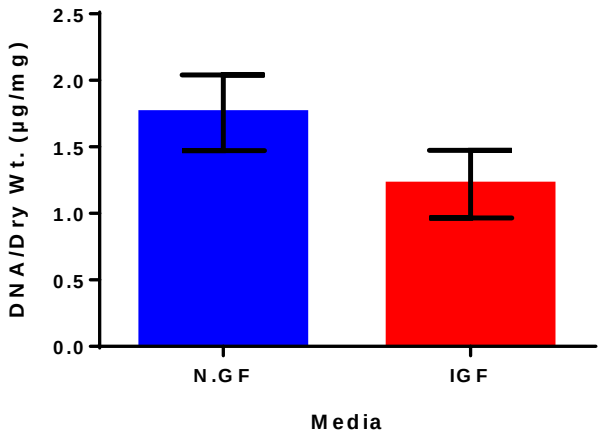

Figure 4.8: Effect of IGF-1 on DNA content

Data presented as mean ± SEM (n=3-8 samples per group).

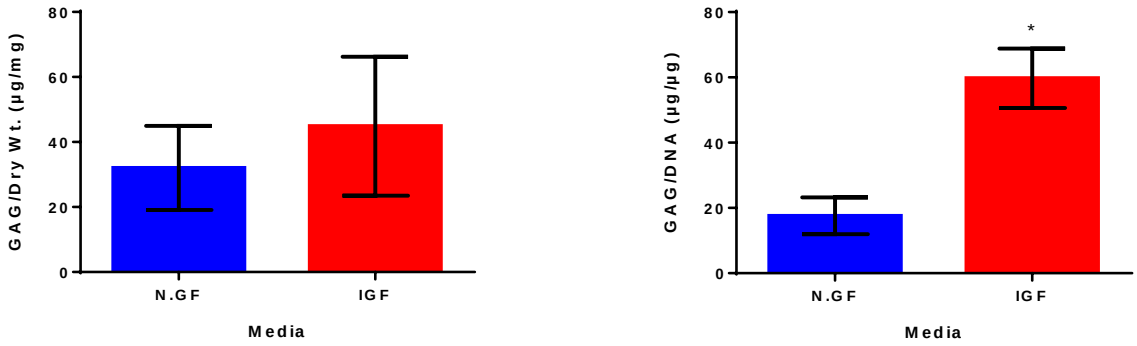

Figure 4.9:Effect of IGF-1 on glycosaminoglycan content

Data presented as mean ± SEM (n=3-9 samples per group). *significant ($p<0.01$).

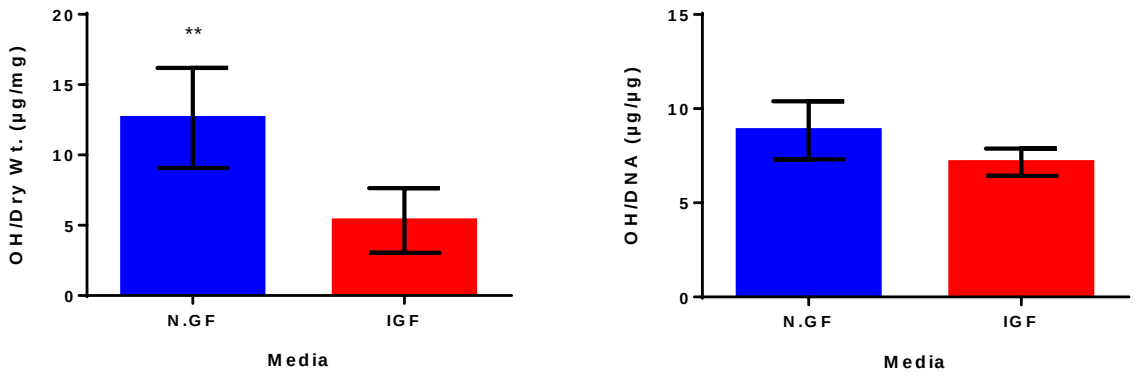

Figure 4.10: Effect of IGF-1 on hydroxyproline content

Data presented as mean ± SEM (n=3-9 samples per group). ** trend (p=0.10).

4.4.2 Histological Evaluation

Cartilaginous samples were stained with safranin O to visualize glycosaminoglycans and sirius red to visualize collagen proteins (Figure 4.11). Morphologically, chondrocytes appeared round in shape and were randomly dispersed throughout the tissue matrix in lacunae, occurring individually or as doubles. Samples without IGF-1 supplementation appeared more cellularly dense compared to the samples supplemented by IGF-1. This trend was also observed biochemically, evidenced by the increased DNA content when normalized to dry weight for samples cultured without growth factors compared to those with IGF-1 supplementation. Positive glycosaminoglycan staining was observed in the safranin O stains of samples both cultured with and without IGF-1, with the samples with IGF-1 supplementation staining more intensely. This was supported by the biochemistry results, where the samples without IGF-1 supplementation exhibited increased glycosaminoglycan content. Since

IGF-1 supplemented samples observed lower cell density, positive glycosaminoglycan staining with safranin O corresponds to the increase in glycosaminoglycan content when normalized to DNA content observed biochemically. Collagen staining with sirius red was significantly more intense in the samples without IGF-1 supplementation, supported by the significant increase in hydroxyproline content observed biochemically when normalized to dry weight. The reduced cellular density observed in the samples with IGF-1 supplementation corresponds to the similar hydroxyproline content between samples when normalized to DNA content. In terms of thickness, samples with IGF-1 supplementation appeared significantly thicker than the samples cultured without growth factors. Overall, IGF-1 supplementation appeared to inhibit cellular proliferation, glycosaminoglycan and collagen synthesis.

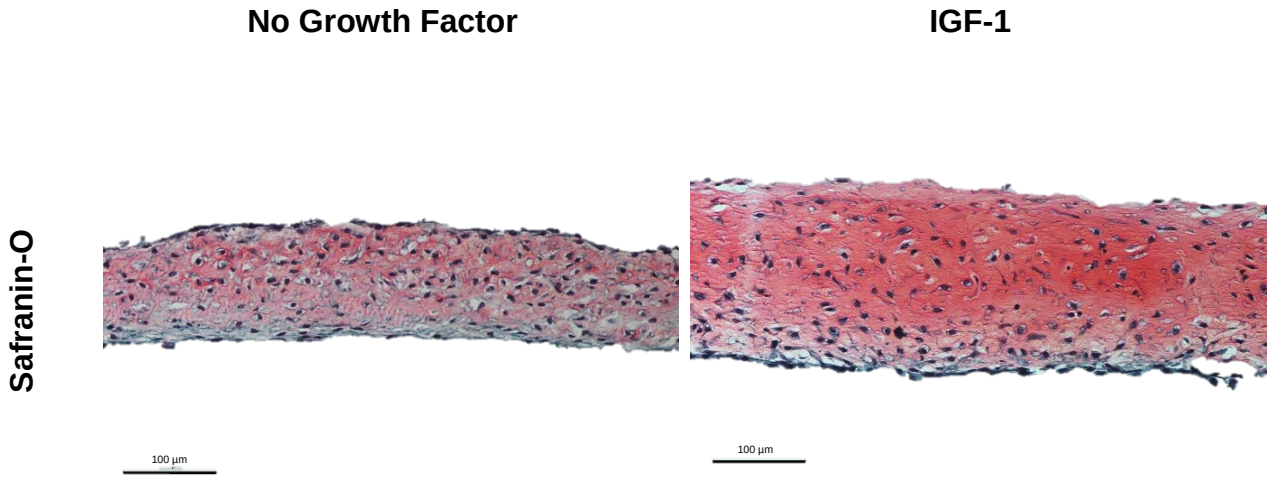

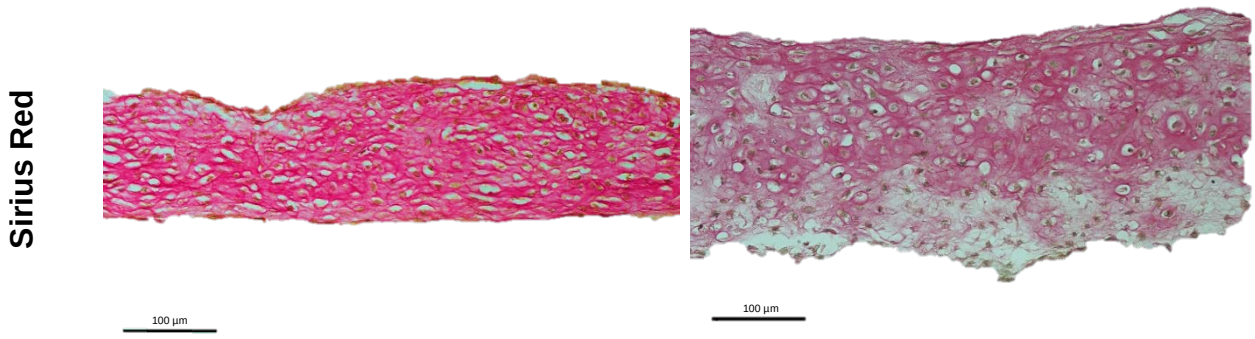

Figure 4.11: Safranin O and Sirius Red staining of cartilaginous tissue with and without IGF-1 supplementation

4.4.3 Mechanical Evaluation

At the end of the culture period, both circumferential and longitudinal strips were taken from the harvested samples for thickness evaluation and tensile testing to determine potential biomechanical differences with respect to direction. For the samples cultured without growth factors, tissue location did not significantly affect the tensile modulus, ultimate tensile strength or ultimate tensile strength. ($p=0.46$, $p=0.26$, $p=0.28$, respectively) (Figure 4.12). For the samples supplemented with IGF-1, strip location also did not significantly affect the tensile modulus, ultimate tensile strength or ultimate tensile strength. ($p=0.37$, $p=0.55$, $p=0.33$, respectively) (Figure 4.13). These results indicated that the cultured tissue was essentially isotropic when cultured with or without growth factors. For this reason, all subsequent results were reported as averages from the longitudinal and circumferential directions.

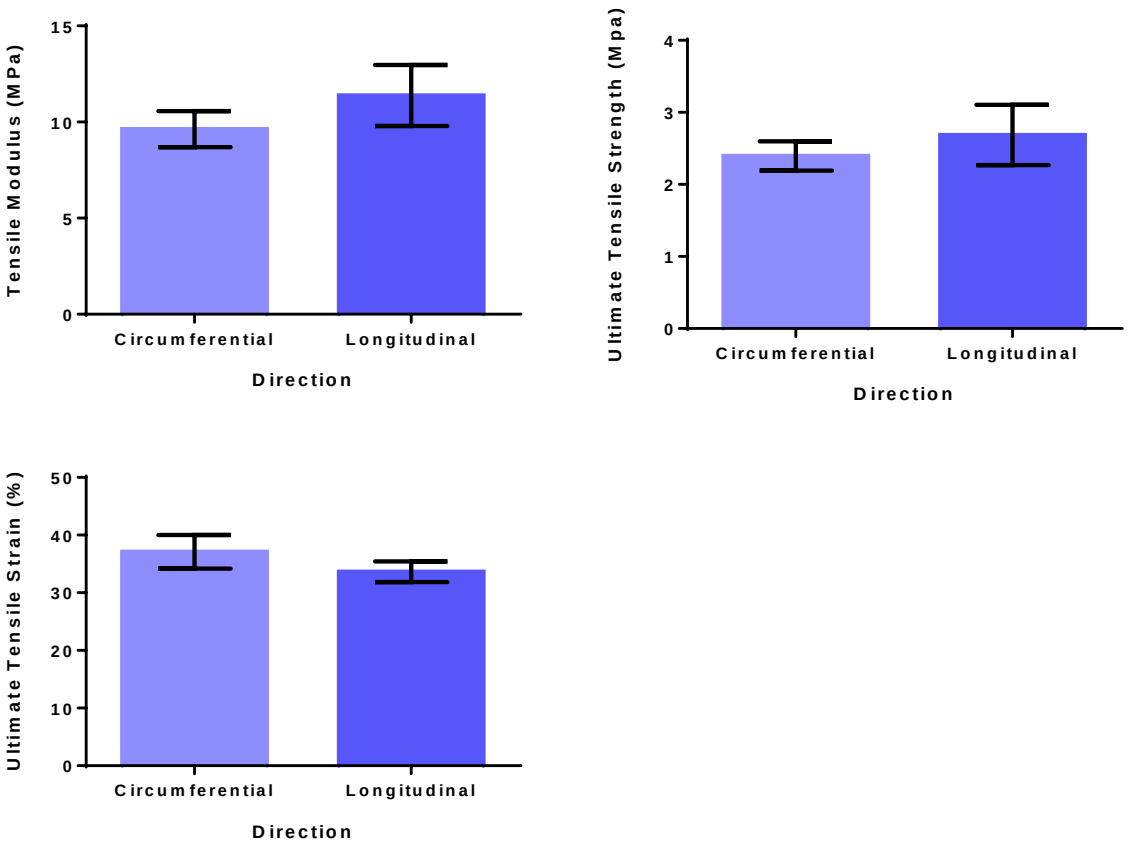

Figure 4.12: The effect of direction on mechanical properties in samples cultured without growth factors

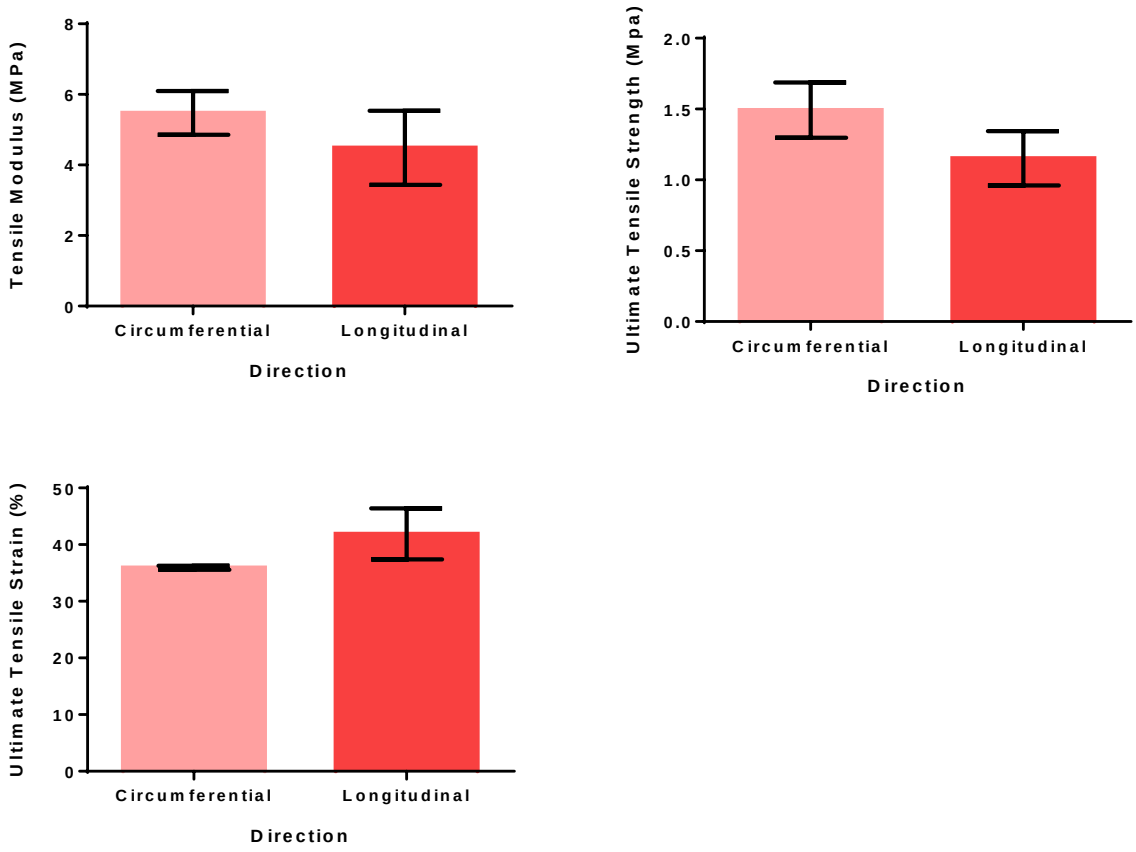

Figure 4.13: The effect of direction on mechanical properties in samples cultured with IGF-1

Comparing the samples cultured with or with growth factors, the samples supplemented with IGF-1 exhibited a significant increase in tissue thickness compared to the control samples without IGF-1 ($p<0.05$) (Figure 4.14). This trend was also observed in the histological evaluation of tissue thickness, with the IGF-1 supplemented samples observed to be thicker than the samples cultured without growth factors. The tensile modulus and ultimate tensile strength were significantly decreased with growth factor

supplementation compared to those cultured without ($p<0.01$ and $p<0.001$ respectively) (Figure 4.14). This trend was also reflected in the biochemically by the increased hydroxyproline content, both when normalized to dry weight and DNA content. The increases hydroxyproline content corresponds to increased collagen content which provided stronger tensile properties. IGF-1 supplementation did not have a significant effect on ultimate tensile strain ($p= 0.78$) (Figure 4.14). Overall, IGF-1 supplementation resulted in thicker tissue with inferior mechanical properties compared to samples cultured without IGF-1, supported by both the biochemical and histological data.

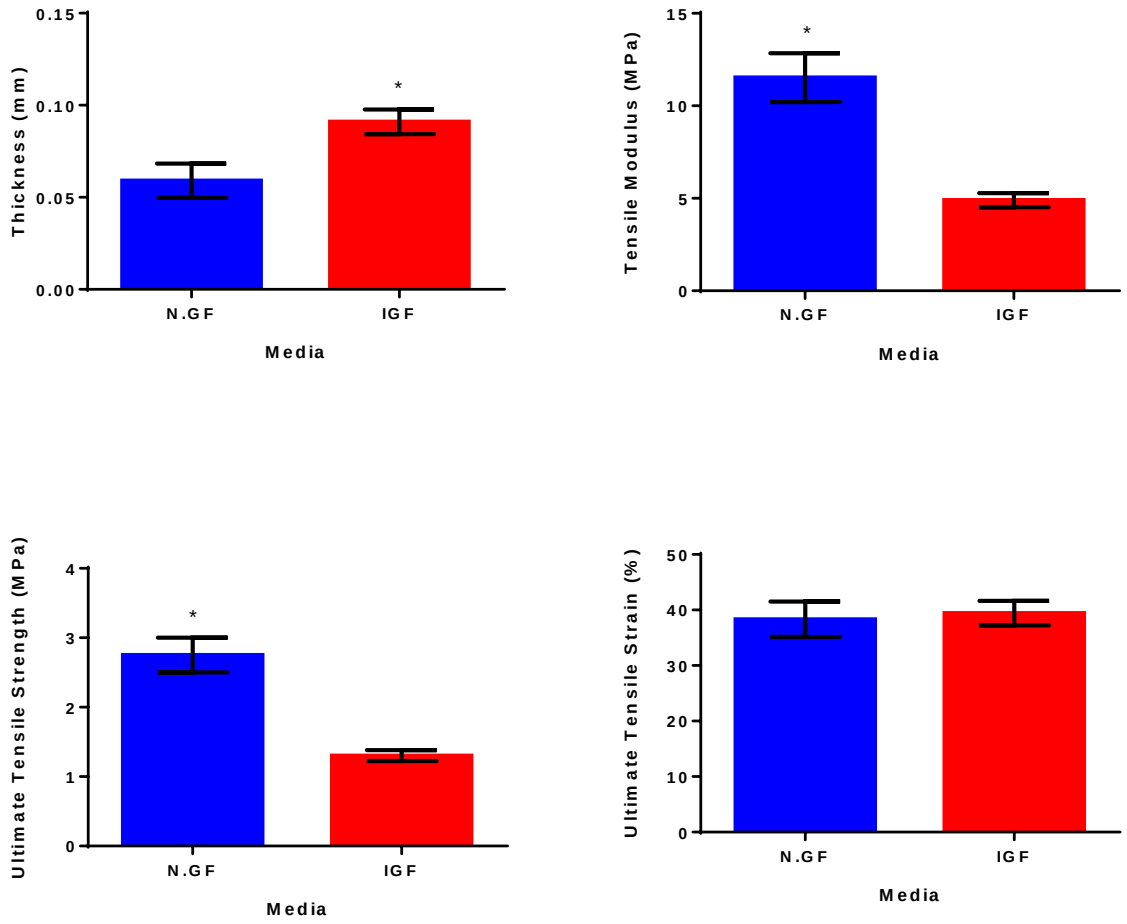

Figure 4.14: Effect of growth factor supplementation on physical properties

Data presented as mean ± SEM (n=3-11 per group). *Significantly different ($p<0.05$).

4.5 Effect of Layering

After the effects of IGF-1 supplementation resulted in thicker tissue but with inferior mechanical properties, the effect of cell layering was investigated. P0 chondrocytes were seeded into the roller tracheal constructs as well as into flasks for expansion. Upon confluence, the plated P0 chondrocytes were trypsinized and the resulting P1

chondrocytes were seeded on top of the P0 chondrocytes within the roller tracheal constructs. Another flask was seeded at this point, and the process was repeated to seed the resulting P2 chondrocytes on top of the P1 and P0 chondrocytes within the roller tracheal constructs. At the end of the 4-week culture period, the chondrocyte-layered constructs were harvested and analyzed biochemically, histologically, and for changes in physical properties. All harvested samples exhibited full coverage of the roller tracheal construct.

4.5.1 Biochemical Evaluation

At the end of the culture period, samples were assayed for DNA, glycosaminoglycan, and hydroxyproline content, with the results normalized to dry weight. Glycosaminoglycan and hydroxyproline content were also normalized to DNA content. Cell layering did not have a significant effect on DNA content ($p=0.12$) (Figure 4.15), although an expected increase in DNA content was observed when layering additional cells onto the roller trachea constructs. Cell layering also did not have a significant effect on glycosaminoglycan or hydroxyproline content when normalized to dry weight ($p=0.98$, $p=0.91$, respectively) (Figure 4.16, Figure 4.17). When glycosaminoglycan content was normalized to DNA content, an observable decrease was observed with chondrocyte layering ($p=0.28$, respectively) (Figure 4.16). This trend was more significant when hydroxyproline content was expressed relative to DNA content, as cell layering significantly decreased hydroxyproline content ($p<0.01$) (Figure 4.17). Overall, chondrocyte layering increased the DNA content observed but did not significantly express glycosaminoglycan and hydroxyproline content when normalized to dry weight.

The observed decreases in glycosaminoglycan and hydroxyproline content when normalized to DNA content correspond to the increased DNA content observed from cell layering.

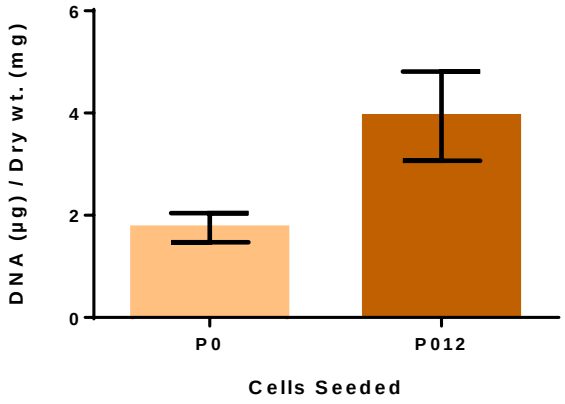

Figure 4.15: Effect of cell layering on DNA content

Data presented as mean ± SEM (n=3-9 samples per group).

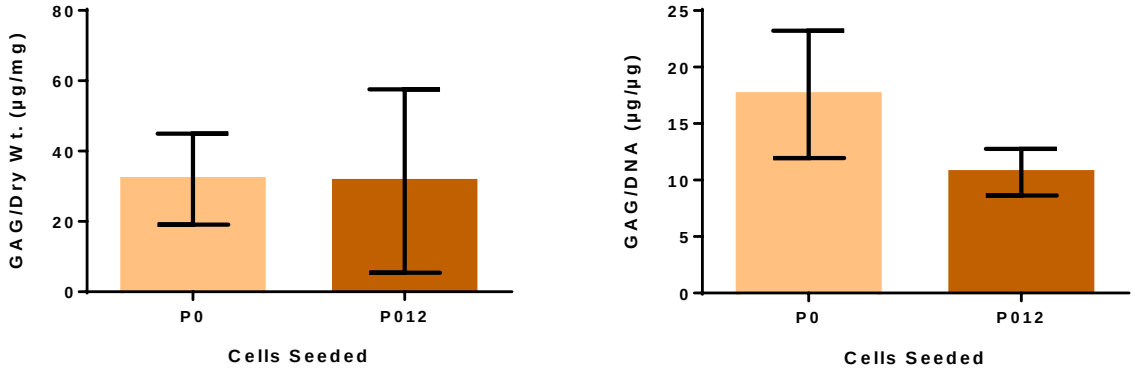

Figure 4.16: Effect of cell layering on glycosaminoglycan content

Data presented as mean ± SEM (n=3-9 samples per group).

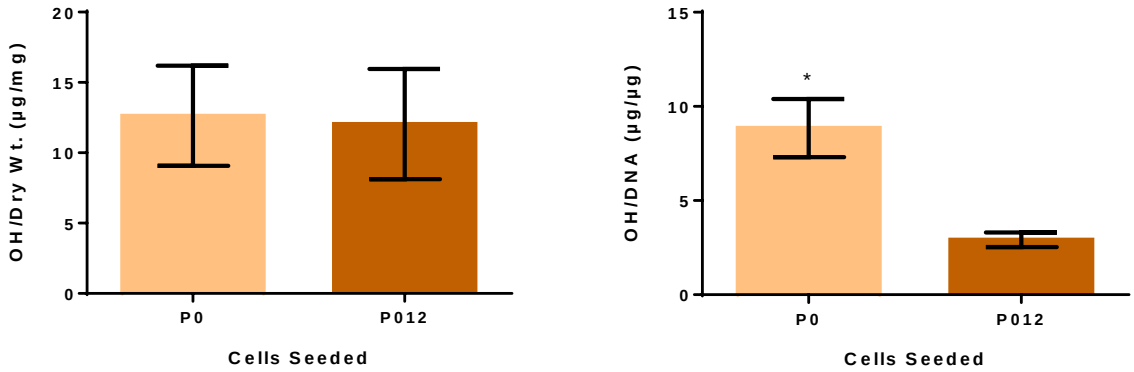

Figure 4.17: Effect of cell layering on hydroxyproline content

Data presented as mean ± SEM (n=3-9 samples per group). *Significant ($p<0.01$).

4.5.2 Histological Evaluation

At the end of the culture period, samples were stained with safranin O and sirius red to visualise glycosaminoglycan content and collagen content, respectively (Figure 4.18). The layered samples appeared to have a higher cellular density, which was supported by the increased DNA content observed biochemically. This was supported by the decrease in glycosaminoglycan and hydroxyproline content when normalize to DNA content as the number of cell present in the layered samples was significantly higher. Morphologically, chondrocytes appeared round in shape and were randomly dispersed throughout the tissue matrix in lacunae for both samples.

Positive glycosaminoglycan staining was observed in both layered and non-layered samples, with non-layered samples staining more intensely. This was supported biochemically, where glycosaminoglycan content was not affected by cell layering when normalized to dry weight. The safranin O stained layered sample in separated into two when sectioning, showing layers of chondrocytes seeded and the variation in the tissue produced. The inner-most tissue was richer in proteoglycans than the outer layer. Collagen staining with sirius red was equally intense for the layered and non-layered samples corresponding to the biochemical results. In terms of thickness, non-layered samples were significantly thicker than the samples cultured without growth factors.

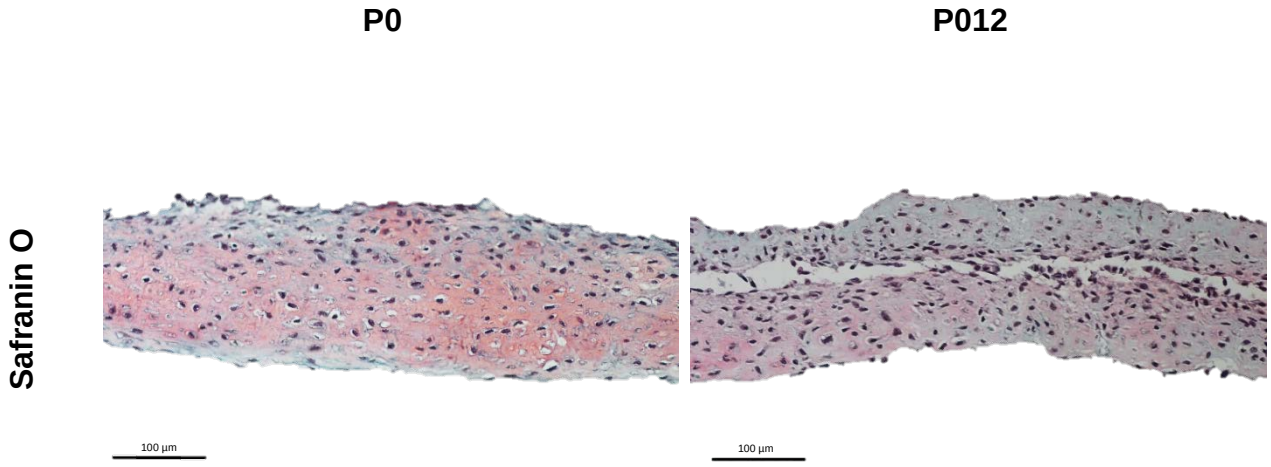

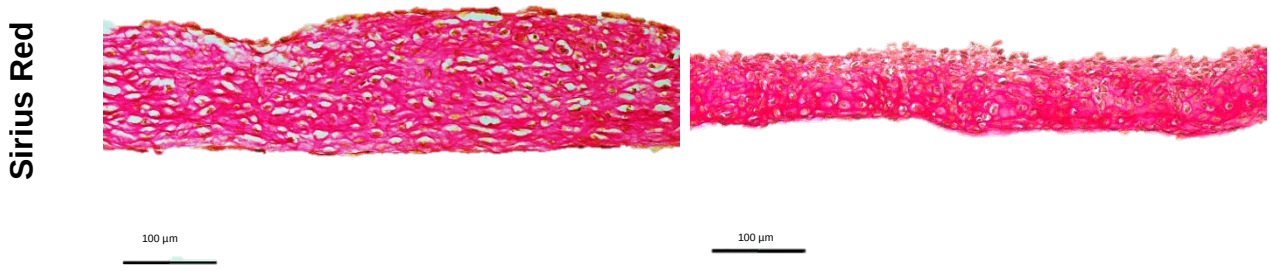

Figure 4.18: Safranin O and Sirius Red staining of non-layered and layered cartilaginous tissue

4.5.3 Mechanical Evaluation

At the end of the culture period, samples were assessed in terms of tissue thickness and biomechanical tensile properties. Non-layered samples were significantly thicker than cells the samples layered with chondrocytes ($p<0.01$) (Figure 4.19). The tensile modulus and ultimate tensile strength were significantly increased by cell layering, ($p<0.01$, $p<0.01$, respectively) (Figure 4.19). This trend was not reflected in the biochemical data, as there was no difference in hydroxyproline content when comparing the layered and non-layered constructs when normalized to dry weight. Increased hydroxyproline content would increase collagen content, which would provide stronger tensile properties. There was no significant effect of cell layering on the ultimate tensile

strain (p=0.53) (Figure 4.19). Overall, cell layering had decreased tissue thickness but increased the tensile properties upon mechanical testing.

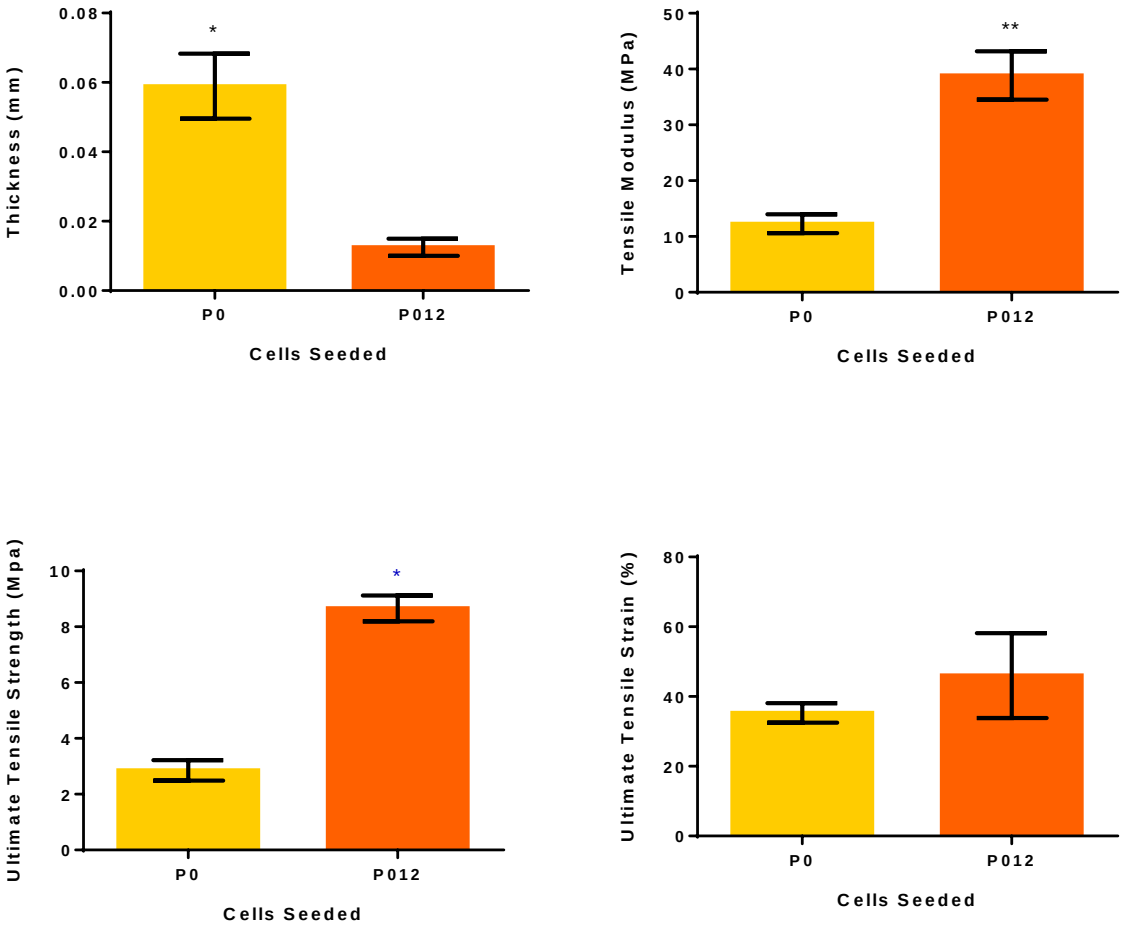

Figure 4.19: The effect of call layering on physical and mechanical properties

5 Discussion

5.1 Chondrocyte Adherence

This experiment was conducted to optimize chondrocyte adherence by varying the inoculation densities. Constructs were seeded under rotation with the seeding media level below the midline of the roller tracheal construct to prevent leaking. Thus, inoculation densities were quantified by volume instead of surface area. The results indicated that the number of live adherent cells plateaued beyond the 3.3×10^5 cells/cm^3 levels. This suggests a limit under the experimental set up where the rotation of the constructs appears to keep cells in suspension and prevent increased chondrocyte adherence beyond this point. This was supported when the final attachment density remained constant as the inoculation density increased and the percentage of live adherent cells from the total cells seeded decreased. All samples were seeded at 0.5 RPM. While this speed was chosen from preliminary studies, seeding at slower rotational speeds may serve to increase chondrocyte adhesion. However, under these conditions the chondrocytes attached to the top of the roller tracheal constructs would be without media for a longer period of time. If the rotational speed was lowered, higher inoculation densities may be effective due to the modified dynamic rolling forces. To facilitate cellular attachment, the roller tracheal constructs utilized plasma-treated polypropylene tubes for chondrocyte attachment. A material with a greater affinity for cellular attachment by increasing hydrophilicity or collagen coating may increase chondrocyte adherence. As the increase in cell density did not increase chondrocyte adherence beyond the density of 3.3×10^5 cells/cm^3, this inoculation density was used for all subsequent experiments.

5.2 Effect of Manual Rotation

The effect of manual rotation was explored to determine its effect on tissue growth. The results indicated that manual rotation did not have a significant effect on tissue growth biochemically. However, differences in tissue coverage of the roller tracheal construct were observed. The samples rotated ½ or ¼ of a rotation at each media exchange always generated full coverage of the roller tracheal construct upon harvest, while non-rotated samples were often void of tissue at the top of the tube (data not shown). The seeded chondrocytes at the top of the roller tracheal construct may have migrated to the bottom of the tube due to gravity or hydrostatic pressure. Thus, regular rotation appears necessary during culture to ensure complete tissue coverage of the construct. However, while no significant differences in tissue biochemistry were observed with manual turning, subsequent experiments focused on automatic rolling.

5.3 Effect of Rotational Speed

Since manual rotation at each media exchange did not significantly affect tissue growth, the effect of automatic rotation was investigated to determine the optimal rotational speed for tissue growth. The bovine articular chondrocytes were dynamically cultured for 4 weeks using a bottle roller to continuously rotate the roller tracheal constructs at either slow (0.1 RPM) or fast (0.5 RPM) rotational speeds.

Both the biochemical and histological results showed minimal differences in DNA and hydroxyproline content with respect to rotational speed. However, there was a significant decrease in glycosaminoglycan content, either by dry weight or DNA content, for samples cultured at 0.5 RPM. This was supported by little to no positive safranin O staining for proteoglycans observed histologically. The differences observed reducing the rotational speed by a factor of 5 likely stem from the fluid-induced shear forces generated by roller bottle culture. The results indicate that slower rotational speeds appear to be optimal for glycosaminoglycan synthesis, with faster rotational speeds limiting glycosaminoglycan synthesis. The increased rotational speed and corresponding shear forces may have washed away glycosaminoglycan content. This has been observed in studies investigating glycosaminoglycan content of chondrocytes under cyclical loading [98]. Samples dynamically cultured at 0.5 RPM not only generated less glycosaminoglycan content than the samples cultured 0.1 RPM, but generated less glycosaminoglycan content than the manually rotated samples when normalized to dry weight. The effect of dynamic culture at 0.5 RPM was also observed histologically in sample thickness, producing much thinner samples than those cultured at 0.1 RPM. These results indicate that continuous culture at 0.5 RPM was not optimal for tissue growth.

Comparing the results of the samples cultured at 0.1 RPM biochemically to that of other species, differences in GAG content but similarities in the DNA and hydroxyproline content were observed when normalized to dry weight. The DNA content (1.48 ± 0.28 µg/mg) was similar to that observed in porcine trachea (1.31 ± 0.27 µg/mg) [99]. The GAG content (32.02 ± 12.92 µg/mg) was 5 times lower than that found in human

trachea (152 ± 18.8 µg/mg) but similar to that of ovine trachea (22 ± 7 µg/mg). The hydroxyproline content (12.63 ± 3.56 µg/mg) was 4 times lower than that found in human trachea (48.3 ± 10.3 µg/mg) but similar that of porcine trachea (8.19 ± 3.19 µg/mg). This was confirmed histologically, where samples rotated at 0.1 RPM stained positive for glycosaminoglycans and hydroxyproline, but not with the intensity observed in native tissue.

In this experimental set up, the roller tracheal constructs sat at the bottom of the vented Bioreaction tubes, with the media level below the midline of the construct to prevent floating. Thus, culture at a slower rotational speeds would leave the chondrocytes attached to the top of the roller tracheal constructs without media for longer periods of time, possibly hindering cell growth. Constructs could also be seeding cells at a slower rotational speed but cultured at higher rotational speed to optimize fluid-induced shear forces for tissue growth. Previous studies have demonstrated that plated chondrocytes increased glycosaminoglycan synthesis in response to fluid-induced shear two-fold [100], [101]. If the roller tracheal construct could be fixed to the middle of the Bioreaction tube, more media could be administered to the samples for increased nutrient delivery and change the shear forces experienced by the chondrocytes to potentially increase tissue growth.

Other studies into the effect of dynamic rotation culture varied greatly in the rotational speed utilized for cell seeding and culture. A similar study which also implemented continuous flow found that a higher RPM increased DNA, glycosaminoglycan, and collagen content; peaking at 15 RPM [88]. In this set-up, constructs were seeded in static culture for 7 days prior to being cultured under in a rotation continuous flow

bioreactor. A rotating double-chamber bioreactor used in clinical trials utilized 5 RPM for seeding and 2 RPM for culture [86], [102]. A longer-term study used a bottle roller for 24-30 weeks with serum-free media and rotated constructs at 10 RPM for the duration of the culture period [103]. Utilizing different rotational speeds could be explored to maximise cellular adhesion at the beginning of culture and then adjusted to maximize tissue growth.

5.4 Effect of Growth Factor Supplementation

Once the rotational speed was optimized at 0.1 RPM, the effect of growth factor supplementation on tissue growth was explored. The bovine articular chondrocytes were dynamically cultured for 4 weeks at 0.1 RPM either with or without Insulin-like growth factor 1 (IGF-1) supplementation.

Samples supplemented with IGF-1 exhibited less DNA content biochemically and decreased cellular density histologically, suggesting that IGF-1 supplementation impaired cell proliferation. The samples supplemented with IGF-1 also exhibited increased glycosaminoglycan content when normalized to either dry weight or DNA content, a trend also observed histologically through safranin O staining. The increased glycosaminoglycan content when normalized to DNA for the IGF-1 supplemented samples corresponds to the decreased cellularity observed biochemically and histologically with IGF-1 supplementation. The decreased cellular density increased the glycosaminoglycan content when expressed relative to DNA content. The samples cultured without growth factors exhibited a significant increase in hydroxyproline content normalized to dry weight compared to the samples cultured without growth factors. This

trend was supported by both the histological and biomechanical data. The samples cultured without growth factors stained more intensely for collagen proteins in sirius red staining, while samples without growth factors exhibited larger tensile modulus and ultimate tensile strength compared to samples cultured with IGF-1 supplementation. Collagen content is predominantly responsible for tensile properties in cartilage tissues [104]. Thus, the increase in the tensile modulus and ultimate tensile strength corresponds to the increased hydroxyproline content observed biochemically and histologically.

The tensile modulus of the samples cultured with and without IGF-1 supplementation (4.90 and 11.52 MPa, respectively) was within the range reported in humans (4.6–13.6 MPa) [99]. The ultimate tensile strength observed in samples with IGF-1 supplementation (1.3 MPa) were consistent with that of other scaffold-free methods (1.1 MPa) [73]. However, the ultimate tensile strength of samples cultured without growth factors was more than twice that of tissue generated with similar scaffold-free methods (2.75 MPa) [73]. IGF-1 supplementation significantly increased tissue thickness, observed both histologically and biomechanically. These results indicate that IGF-1 supplementation increased cellularity and glycosaminoglycan synthesis, but decreased collagen synthesis, leading to tissue with inferior mechanical properties. The increased glycosaminoglycan content may have attracted additional water which may have caused the tissue to swell restringing in a larger thickness. The indifference in mechanical properties in the circumferential and longitudinal directions was unexpected given direction of the fluid-induced shear forces generated from roller bottle culture. Physiologically, the trachea’s tensile properties in the circumferential direction are

increased for the functions of inhalation and exhalation [105]. As this indifference was observed in both samples cultured with and without growth factors, the tissue produced by roller bottle culture at 0.1 RPM was essentially homogeneous and isotropic. This agrees with literature that found no significant difference in longitudinal versus circumferential biomechanical properties in a seeded scaffold with respect to suture retention[105]. Other studies have found out that cultured tissue to be anisotropic, showing a higher elastic moduli longitudinally [99], [106].

While this experiment only examined tensile biomechanical properties, functional biomechanical measurements such as burst pressure should be considered to evaluate physiologically relevant loads. As the trachea is circumferentially strong in tension for respiration and in compression to prevent airway collapse [105], strategies to increase these properties in cultured tissue should be implemented. Overall, IGF-1 supplementation produced thicker tissue with increased cellularity but with inferior mechanical properties compared to the tissue cultured without growth factors. This was evidenced by decreased DNA, glycosaminoglycan and hydroxyproline content observed in the IGF-1 supplemented samples when normalized to dry weight.

Transforming growth factor beta 1 (TGF-β1) is often used to enhance mechanical properties in scaffold-free tissues [107]. However, TGF-β1 supplementation in static culture with manual rotation at each media exchange resulted in tissues collapsing upon themselves before the end of the culture period (data not shown). As such, stimulation with TGF-β1 was not explored further and IGF-1 was administered to samples instead. Previous work has demonstrated that a combination of TGF-1 with BMP-2 doubled glycosaminoglycan content and the aggregate modulus in neocartilage [80]. Thus, a

combination of growth factors could be explored to enhance tissue formation and properties. Similarly, previous studies have explored the use of enzymes such as chondroitinase-ABC (C-ABC) to digest glycosaminoglycans to improve collagen synthesis, as too much glycosaminoglycan content may impair collagen synthesis and reduce biomechanical properties [108]. Controlled supplementation of C-ABC could be explored to increase the tensile modulus, which was observed to increase by 80% with admiration halfway through the culture period [109]. Other studies have explored the use of lysyl-oxidase (LOX) to initiate collagen fibril cross-linking [110]. Also, the combination of LOX and C-ABC resulted over a 200% increase in the tensile modulus and ultimate tensile strength of the neocartilage [110]. Overall, the combination of additional growth factors and/or enzymes at various points throughout the culture period may optimise tissue mechanical properties.

5.5 Effect of Layering

With the effect of growth factor supplementation determined, the effect of cell layering was investigated. P0 chondrocytes were seeded into the roller tracheal constructs as well as into flasks for expansion. Upon confluence, the plated P0 chondrocytes were trypsinized and the resulting P1 chondrocytes were seeded on top of the P0 chondrocytes within the roller tracheal constructs. This process was repeated for the resulting P2 cells.

The results indicated that chondrocyte layering increased the cellularity of the samples, observed biochemically with DNA content and histologically with visualized cellular density. These results were expected from layering additional chondrocytes onto the

roller tracheal constructs. From the constant inoculation density and low, if any, cell counts of the effluent seeding media, it was assumed that the same number of cells adhered to the roller tracheal construct each layering. The initial P0 layer of cells would be attracted to the plasma-treated, hydrophilic polypropylene surface of the roller tracheal constructs, and each subsequent layer of P1 and P2 chondrocytes would adhere to the extracellular matrix produced by the P0 cells, acting as anchor points. Harvesting samples after each layering would confirm the effect of each layering. Chondrocyte layering did not effect on glycosaminoglycan and hydroxyproline content when normalized to dry weight. This trend was observed in the sirius red staining for collagen content, where both samples stained with equal intensity. Equal glycosaminoglycan staining was not observed in the safranin O staining. However, the sample was separated when sectioning with the inner-most tissue exhibiting similar proteoglycans staining to the unlayered samples. The glycosaminoglycan and hydroxyproline content of the samples when normalized to DNA content decreased for the layered samples, which corresponds to the equal amounts of glycosaminoglycan and hydroxyproline relative to dry weight observed with the increased DNA content. Cell layered decreased tissue thickness, observed both histologically and through biomechanical testing. Despite this, chondrocyte layering increased the tensile modulus and ultimate tensile strength. The ultimate tensile strain was unaffected by cell layering.

The layering of additional chondrocytes may have skewed the biochemistry data, as newly added chondrocytes may not have produced additional extracellular matrix but affected the data normalized to DNA content. Furthermore, there is extensive literature on the effect of passaging on chondrocyte differentiation [111]. While previous research

indicated that chondrocytes could be expanded to four passages without permanent dedifferentiation [112], other studies show that gene expression was affected more rapidly [113]. Thus, the additionally seeded chondrocytes may not have contributed to the extracellular matrix of the construct as they were passaged prior to layering. Immunohistochemical analysis of collagen II and collagen I would determine if the passaged chondrocytes dedifferentiated before prior to layering, as dedifferentiation would be marked by an increase in collagen I production and a decrease in collagen II production as chondrocytes regress. There have been various methods to maintain chondrocyte phenotype during expansion[114]–[117], which could be used in conjunction with cell layering to optimize tissue growth in roller bottle culture.

Layered samples may also have been affected by the re-seeding process, where the roller tracheal construct were capped and only given 1 mL of seeding media compared to the 15 mL of culture media given to promote tissue growth. This may have hindered tissue growth due to the lack of nutrients available from the smaller volume of media. As such, a longer culture period or a smaller seeding period may be optimal for tissue growth to prevent nutrient deprival. Additionally, a slower rotational speed during re-seeding may be investigated, though this would leave the cells at the top of the construct are without media for a longer period of time.

5.6 Limitations of the study

In all experiments, samples were cultured in plasma-treated polypropylene tubes. However, a more hydrophilic material may facilitate greater cell attachment and tissue growth. Furthermore, all experiments seeded roller tracheal constructs with

chondrocytes while under rotation at 0.5 RPM. This rotational speed, the slowest offered by the bottle roller, may have limited cellular attachment to the roller tracheal constructs and kept the cells in suspension. Additionally, media levels were kept below the midline of constructs during seeding to prevent leaking, possibly limiting cellular attachment.

During static culture with manual rotation at each media exchange, samples were limited to 5 mL of culture media, which may not be sufficient for tissue growth at this cellular density as the media may be depleted of nutrients too quickly. In dynamic roller culture, samples were limited to 15 mL of culture media due to the experimental set up to prevent floating. Fixing the constructs in place within the Bioreation tubes would allow more media to be administered to the samples during culture. Samples were also limited in their exposure to media, as the top half of the tubes were not in contact with media during dynamic rotational culture. The lowest rotational speed attainable in the experimental set up was 0.1 RPM, dictated by the space available on the bottle roller and materials available to expand the width of the roller tracheal constructs. Culture at a slower speed may induce greater tissue growth. Furthermore, samples were cultured at one rotational speed for the duration of the culture period. Investigation into which rotational speed may be optimal for cellular attachment and for tissue growth would be optimal. Layered samples may also have been affected by the laying process, where roller tracheal construct were capped and only given 1 mL of seeding media compared to the 15 mL of media given to samples during culture. Due to size constraints of the bottle roller, the attachments needed to scale down the rotational speed, and the incubator housing all components, a low throughput of samples during experiments

were observed for each individual experiment. Furthermore, there was high variability in the biochemical results of samples within the same experiment, likely due to variation in the animals harvested.

6 Conclusion and Recommendations

6.1 Conclusions

The purpose of this study was to create a seamless cartilage cylinder for tracheal tissue engineering using scaffold-free techniques and roller bottle culture *in vitro*. First, chondrocyte adherence was optimized based on the experimental set up, where seeding additional cells beyond a certain point did not increase cellular attachment. In static culture, manual rotation at each media exchange demonstrated little difference between samples rotated ½ or ¼ of a turn. However, rotation was necessary to ensure full tissue coverage of the roller tracheal constructs, as non-rotated samples were often void of tissue at the top of the tube. When scaling up to dynamic culture with automatic rotation, samples cultured at a slower rotational seed produced thicker tissues with an exchanged extracellular matrix upon harvest. A significant reduction in glycosaminoglycan content was observed in samples cultured at a faster rotational speed, observed both biochemically and histologically. This may be due to the increased fluid-induced forces experienced by the tissue, possibly washing away glycosaminoglycan content at the higher rotational speeds. Because of the increased tissue accumulation observed at slow (0.1 RPM) rotational speed, all subsequent experiments were cultured at 0.1 RPM. The supplementation of IGF-1 resulted in thicker tissue accompanied by decreased DNA, glycosaminoglycan, and hydroxyproline content compared to samples cultured without growth factors. Furthermore, IGF-1 supplemented samples exhibited inferior biomechanical properties. Chondrocyte layering produced thinner tissue with a similar extracellular matrix, but enhanced biomechanical properties. Overall, the experiments were successfully demonstrated the

potential of scaffold-free tissue engineering using roller bottle culture to generate seamless cylindrical cartilage constructs for long-segment tracheal replacement. However, further improvements must be made to experimental design to produce better quality cartilaginous tissues.

6.2 Recommendations

Further work must be carried out to gain a deeper understanding of how roller bottle culture affects cartilage growth for tracheal replacements. Though chondrocyte adherence was optimized in this experimental set up, a slower rotational speed with a more hydrophilic material may increase chondrocyte adherence. Since slower rotational speeds generated enhanced cartilaginous samples biochemically and histologically, culture at an even slower rotational speed may induce greater tissue growth. Furthermore, optimizing the rotational speed for cellular adherence and then again for tissue growth may generate improved tracheal constructs. As Insulin-like growth factor 1 (IGF-1) supplementation generated thicker, glycosaminoglycan-rich tissue with inferior mechanical properties, the incorporation of other growth factors and/or enzymes may promote tracheal tissue regeneration. Finally, layering cells expended through methods that maintain chondrocyte phenotype may strengthen the extracellular matrix of the cartilaginous tracheal tissue.

References

[1] C. Crowley, M. Birchall, and A. M. Seifalian, *Trachea transplantation: From laboratory to patient*, vol. 9, no. 4. 2015, pp. 357–367.

[2] P. Lange, J. M. Fishman, M. J. Elliott, P. De Coppi, and M. A. Birchall, “What Can Regenerative Medicine Offer for Infants with Laryngotracheal Agenesis?,” *Otolaryngol. -- Head Neck Surg.*, vol. 145, no. 4, pp. 544–550, 2011.

[3] E. Maughan, F. Lesage, C. R. Butler, R. E. Hynds, R. Hewitt, S. M. Janes, J. A. Deprest, and P. De Coppi, “Airway tissue engineering for congenital laryngotracheal disease,” *Semin. Pediatr. Surg.*, vol. 25, no. 3, pp. 186–190, 2016.

[4] A. Napieralska, L. Miszczyk, and S. Blamek, “Tracheal cancer – treatment results, prognostic factors and incidence of other neoplasms,” *Radiol. Oncol.*, vol. 50, no. 4, pp. 4–7, 2016.

[5] R. Cotton, “Management of subglottic stenosis in infancy and childhood. Review of a consecutive series of cases managed by surgical reconstruction,” *Ann. Otol. Rhinol. Laryngol.*, vol. 87, no. 5 I, pp. 649–657, Sep. 1978.

[6] R. Farzanegan, B. Farzanegan, M. Zangi, M. Golestani Eraghi, S. Noorbakhsh, N. Doozandeh Tabarestani, and M. B. Shadmehr, “Incidence Rate of Post-Intubation Tracheal Stenosis in Patients Admitted to Five Intensive Care Units in Iran,” *Iran. Red Crescent Med. J.*, vol. 18, no. 9, 2016.

[7] A. Sarper, A. Ayten, I. Eser, O. Ozbudak, and A. Demircan, “Tracheal stenosis aftertracheostomy or intubation: review with special regard to cause and

management.,” *Texas Hear. Inst. J.*, vol. 32, no. 2, pp. 154–8, 2005.

[8] J. P. Jacobs, J. A. Quintessenza, L. M. Botero, H. M. Van Gelder, J. M. Giroud, M. J. Elliott, and C. Herberhold, “The role of airway stents in the management of pediatric tracheal, carinal, and bronchial disease,” *Eur. J. Cardio-thoracic Surg.*, vol. 18, no. 5, pp. 505–512, 2000.

[9] H. C. Grillo, “Tracheal replacement: a critical review,” *Ann. Thorac. Surg.*, vol. 73, no. 6, pp. 1995–2004, 2002.

[10] C. R. Butler, S. Speggiorin, F. M. Rijnberg, D. J. Roebuck, N. Muthialu, R. J. Hewitt, and M. J. Elliott, “Outcomes of slide tracheoplasty in 101 children: A 17-year single-center experience,” *J. Thorac. Cardiovasc. Surg.*, vol. 147, no. 6, pp. 1783–1789, 2014.

[11] E. M., H. B.E.J., and W. C., “Slide tracheoplasty,” *Current Opinion in Otolaryngology and Head and Neck Surgery*, vol. 16, no. 1. pp. 75–82, 2008.

[12] S. Haykal, M. Salna, T. K. Waddell, and S. O. Hofer, “Advances in Tracheal Reconstruction,” *Plast. Reconstr. Surg. – Glob. Open*, vol. 2, no. 7, p. e178, 2014.

[13] J. Volmerig and E. Hecker, “Reconstruction of the trachea,” *Minerva Pneumol.*, vol. 53, no. 2, pp. 47–58, Dec. 2014.

[14] N. Okumura, T. Nakamura, T. Natsume, K. Tomihata, Y. Ikada, and Y. Shimizu, “Experimental study on a new tracheal prosthesis made from collagen-conjugated mesh.,” *J. Thorac. Cardiovasc. Surg.*, vol. 108, no. 2, pp. 337–45, 1994.

[15] T. Ishimaru, M. Komura, M. Sugiyama, H. Komura, M. Arai, J. Fujishiro, C. Uotani,

K. Miyakawa, T. Kakihara, K. Hoshi, T. Takato, Y. Tabata, H. Komuro, and T. Iwanaka, “Slow release of basic fibroblast growth factor (b-FGF) enhances mechanical properties of rat trachea,” *J. Pediatr. Surg.*, vol. 50, no. 2, pp. 256–259, 2015.

[16] J. H. Lee, H. S. Park, S. H. Oh, J. H. Lee, J. R. Kim, H. J. Kim, S. Y. Jung, S. M. Chung, H. S. Choi, and H. S. Kim, “Triple-layered polyurethane prosthesis with wrinkles for repairing partial tracheal defects,” *Laryngoscope*, vol. 124, no. 12, pp. 2757–2763, 2014.

[17] A. Tani, Y. Tada, T. Takezawa, I. Wada, M. Imaizumi, Y. Nomoto, M. Nomoto, and K. Omori, “Regenerative process of tracheal epithelium using a collagen vitrigel sponge scaffold,” *Laryngoscope*, vol. 123, no. 6, pp. 1469–1473, 2013.

[18] Y. Tada, T. Takezawa, A. Tani, T. Nakamura, and K. Omori, “Collagen vitrigel scaffold for regenerative medicine of the trachea: Experimental study and quantitative evaluation,” *Acta Otolaryngol.*, vol. 132, no. 4, pp. 447–52, 2012.

[19] Y. Tatekawa, N. Kawazoe, G. Chen, Y. Shirasaki, H. Komuro, and M. Kaneko, “Tracheal defect repair using a PLGA-collagen hybrid scaffold reinforced by a copolymer stent with bFGF-impregnated gelatin hydrogel,” *Pediatr. Surg. Int.*, vol. 26, no. 6, pp. 575–580, 2010.

[20] H. Igai, S. S. Chang, M. Gotoh, Y. Yamamoto, M. Yamamoto, Y. Tabata, and H. Yokomise, “Widespread and Early Tracheal Cartilage Regeneration by Synchronous Slow Release of b-FGF and BMP-2,” *ASAIO J.*, vol. 55, no. 3, pp. 266–270, 2009.

[21] B. Ekser, M. Ezzelarab, H. Hara, D. J. Van Der Windt, M. Wijkstrom, R. Bottino, M. Trucco, and D. K. C. Cooper, “Clinical xenotransplantation: The next medical revolution?,” *Lancet*, vol. 379, no. 9816, pp. 672–683, 2012.

[22] P. Delaere, J. Vrancks, G. Verleden, P. De Leyn, D. D. Van Raemdonck, J. Vranckx, G. Verleden, P. De Leyn, and D. D. Van Raemdonck, “Tracheal allotransplantation after withdrawal of immuno-suppressive therapy,” *Bull. L Acad. Natl. Med.*, vol. 194, no. 7, pp. 138–45, 2010.

[23] P. R. Delaere, J. J. Vranckx, J. Meulemans, V. Vander Poorten, K. Segers, D. Van Raemdonck, P. De Leyn, H. Decaluwé, C. Dooms, and G. Verleden, “Learning curve in tracheal allotransplantation,” *Am. J. Transplant.*, vol. 12, no. 9, pp. 2538–2545, 2012.

[24] J. M. Fishman, K. Wiles, M. W. Lowdell, P. De Coppi, M. J. Elliott, A. Atala, and M. A. Birchall, “Airway tissue engineering: an update,” *Expert Opin. Biol. Ther.*, vol. 14, no. 10, pp. 1477–1491, 2014.

[25] C. C. Reynolds, S. a Martinez, A. Furr, M. Cunningham, J. M. Bumpous, E. J. Lentsch, J. C. Banis, D. Vasilic, B. Storey, O. Wiggins, C. Maldonado, G. Perez-Abadia, and J. H. Barker, “Risk acceptance in laryngeal transplantation.,” *Laryngoscope*, vol. 116, no. 10, pp. 1770–5, 2006.

[26] G. M. Roomans, “Tissue Engineering and the Use of Stem / Progenitor Cells for Airway Epithelium Repair,” *Eur. cells Mater.*, vol. 19, pp. 284–299, 2010.

[27] M. Kalathur, S. Baiguera, and P. Macchiarini, “Translating tissue-engineered tracheal replacement from bench to bedside,” *Cell. Mol. Life Sci.*, vol. 67, pp.

4185–4196, 2010.

[28] J. Raghunath, J. Rollo, K. M. Sales, P. E. Butler, and A. M. Seifalian, “Biomaterials and scaffold design: key to tissue-engineering cartilage,” *Biotechnol. Appl. Biochem.*, vol. 46, no. Pt 2, pp. 73–84, 2007.

[29] A. J. Sophia Fox, A. Bedi, and S. A. Rodeo, “The basic science of articular cartilage: structure, composition, and function.,” *Sports Health*, vol. 1, no. 6, pp. 461–8, Nov. 2009.

[30] S. Haykal, J. P. Soleas, M. Salna, S. O. P. Hofer, and T. K. Waddell, “Evaluation of the Structural Integrity and Extracellular Matrix Components of Tracheal Allografts Following Cyclical Decellularization Techniques: Comparison of Three Protocols,” *Tissue Eng. Part C Methods*, vol. 18, no. 8, pp. 614–623, 2012.

[31] M. C. Jones, F. A. Rueggeberg, A. J. Cunningham, H. A. Faircloth, T. Jana, D. Mettenburg, J. L. Waller, G. N. Postma, and P. M. Weinberger, “Biomechanical changes from long-term freezer storage and cellular reduction of tracheal scaffoldings,” *Laryngoscope*, vol. 125, no. 1, pp. E16–E22, 2015.

[32] Y. Chae, D. Protsenko, P. K. Holden, C. Chlebicki, and B. J. F. Wong, “Thermoforming of tracheal cartilage: Viability, shape change, and mechanical behavior,” *Lasers Surg. Med.*, vol. 40, no. 8, pp. 550–561, 2008.

[33] S. L. Bogan, G. Z. Teoh, and M. A. Birchall, “Tissue Engineered Airways: A Prospects Article,” *J. Cell. Biochem.*, vol. 117, no. 7, pp. 1497–1505, 2016.

[34] P. Macchiarini, P. Jungebluth, T. Go, M. A. Asnaghi, L. E. Rees, T. A. Cogan, A.

Dodson, J. Martorell, S. Bellini, P. P. Parnigotto, S. C. Dickinson, A. P. Hollander, S. Mantero, M. T. Conconi, and M. A. Birchall, “Clinical transplantation of a tissue-engineered airway.,” *Lancet*, vol. 372, no. 9655, pp. 2023–30, Dec. 2008.

[35] A. Gonfiotti, M. O. Jaus, D. Barale, S. Baiguera, C. Comin, F. Lavorini, G. Fontana, O. Sibila, G. Rombol??, P. Jungebluth, P. MacChiarini, A. G. Otti, M. O. Jaus, D. Barale, S. Baiguera, C. Comin, F. Lavorini, G. Fontana, O. Sibila, *et al.*, “The first tissue-engineered airway transplantation: 5-year follow-up results,” *Lancet*, vol. 383, no. 9913, pp. 238–244, 2014.

[36] M. J. Elliott, P. De Coppi, S. Speggiorin, D. Roebuck, C. R. Butler, E. Samuel, C. Crowley, C. McLaren, A. Fierens, D. Vondrys, L. Cochrane, C. Jephson, S. Janes, N. J. Beaumont, T. Cogan, A. Bader, A. M. Seifalian, J. J. Hsuan, M. W. Lowdell, *et al.*, “Stem-cell-based, tissue engineered tracheal replacement in a child: A 2-year follow-up study,” *Lancet*, vol. 380, no. 9846, pp. 994–1000, 2012.

[37] N. J. Hamilton, M. Kanani, D. J. Roebuck, R. J. Hewitt, R. Cetto, E. J. Culme-Seymour, E. Toll, A. J. Bates, A. P. Comerford, C. A. McLaren, C. R. Butler, C. Crowley, D. McIntyre, N. J. Sebire, S. M. Janes, C. O’Callaghan, C. Mason, P. De Coppi, M. W. Lowdell, *et al.*, “Tissue-Engineered Tracheal Replacement in a Child: A 4-Year Follow-Up Study,” *Am. J. Transplant.*, vol. 15, no. 10, pp. 2750–2757, 2015.

[38] A. Weymann, N. P. Patil, A. Sabashnikov, S. Korkmaz, S. Li, P. Soos, R. Ishtok, N. Chaimow, I. P??tzold, N. Czerny, B. Schmack, A. F. Popov, A. R. Simon, M. Karck, and G. Szabo, “Perfusion-Decellularization of Porcine Lung and Trachea

for Respiratory Bioengineering," *Artif. Organs*, vol. 39, no. 12, pp. 1024–1032, 2015.

[39] S. Haykal, Y. Zhou, P. Marcus, M. Salna, T. Machuca, S. O. P. Hofer, and T. K. Waddell, "The effect of decellularization of tracheal allografts on leukocyte infiltration and of recellularization on regulatory T cell recruitment," *Biomaterials*, vol. 34, no. 23, pp. 5821–5832, 2013.

[40] P. M. Crapo, T. W. Gilbert, and S. F. Badylak, "An overview of tissue and whole organ decellularization processes," *Biomaterials*, vol. 32, no. 12, pp. 3233–3243, 2011.

[41] T. W. Gilbert, T. L. Sellaro, and S. F. Badylak, "Decellularization of tissues and organs," *Biomaterials*, vol. 27, no. 19, pp. 3675–3683, 2006.

[42] P. Jungebluth, T. Go, A. Asnaghi, S. Bellini, J. Martorell, C. Calore, L. Urbani, H. Ostertag, S. Mantero, M. T. Conconi, and P. Macchiarini, "Structural and morphologic evaluation of a novel detergent-enzymatic tissue-engineered tracheal tubular matrix," *J. Thorac. Cardiovasc. Surg.*, vol. 138, no. 3, pp. 586–593, 2009.

[43] S. Baiguera, C. Del Gaudio, E. Kuevda, A. Gonfiotti, A. Bianco, and P. Macchiarini, "Dynamic decellularization and cross-linking of rat tracheal matrix," *Biomaterials*, vol. 35, pp. 6344–6350, 2014.

[44] F. Sun, Y. Jiang, Y. Xu, H. Shi, S. Zhang, X. Liu, S. Pan, G. Ye, W. Zhang, F. Zhang, and C. Zhong, "Genipin cross-linked decellularized tracheal tubular matrix for tracheal tissue engineering applications.," *Sci. Rep.*, vol. 6, no. September 2015, p. 24429, 2016.

[45] S. Baiguera, C. Del Gaudio, M. O. Jaus, L. Polizzi, A. Gonfiotti, C. E. Comin, A. Bianco, D. Ribatti, D. A. Taylor, and P. Macchiarini, “Long-term changes to in vitro preserved bioengineered human trachea and their implications for decellularized tissues,” *Biomaterials*, vol. 33, no. 14, pp. 3662–3672, 2012.

[46] A. M. Kajbafzadeh, S. Sabetkish, N. Sabetkish, S. Muhammadnejad, A. Akbarzadeh, S. M. Tavangar, M. J. Mohseni, and S. Amanpour, “In-vivo trachea regeneration: fabrication of a tissue-engineered trachea in nude mice using the body as a natural bioreactor,” *Surg. Today*, vol. 45, no. 8, pp. 1040–1048, 2014.

[47] S. F. Badylak, D. J. Weiss, A. Caplan, and P. MacChiarini, “Engineered whole organs and complex tissues,” *Lancet*, vol. 379, no. 9819, pp. 943–952, 2012.

[48] K. Kojima and C. a. Vacanti, “Tissue engineering in the trachea,” *Anat. Rec.*, vol. 297, no. September 2013, pp. 44–50, Jan. 2014.

[49] K. Omori, Y. Tada, T. Suzuki, Y. Nomoto, T. Matsuzuka, K. Kobayashi, T. Nakamura, S. Kanemaru, M. Yamashita, and R. Asato, “Clinical application of in situ tissue engineering using a scaffolding technique for reconstruction of the larynx and trachea,” *Ann. Otol. Rhinol. Laryngol.*, vol. 117, no. 9, pp. 673–678, 2008.

[50] P. Jungebluth, E. Alici, S. Baiguera, K. Le Blanc, P. Blomberg, B. Bozóky, C. Crowley, O. Einarsson, K. H. Grinnemo, T. Gudbjartsson, S. Le Guyader, G. Henriksson, O. Hermanson, J. E. Juto, B. Leidner, T. Lilja, J. Liska, T. Luedde, V. Lundin, *et al.*, “Tracheobronchial transplantation with a stem-cell-seeded bioartificial nanocomposite: A proof-of-concept study,” *Lancet*, vol. 378, pp. 1997–

2004, 2011.

[51] Y. Farhatnia, A. Tan, A. Motiwala, B. G. Cousins, and A. M. Seifalian, “Evolution of covered stents in the contemporary era: Clinical application, materials and manufacturing strategies using nanotechnology,” *Biotechnol. Adv.*, vol. 31, no. 5, pp. 524–542, 2013.

[52] A. M. Seifalian, H. J. Salacinski, A. Tiwari, A. Edwards, S. Bowald, and G. Hamilton, “In vivo biostability of a poly(carbonate-urea)urethane graft,” *Biomaterials*, vol. 24, no. 14, pp. 2549–2557, 2003.

[53] J. X. Law, L. L. Liau, B. S. Aminuddin, and B. H. I. Ruszymah, “Tissue-engineered trachea: A review,” *Int. J. Pediatr. Otorhinolaryngol.*, vol. 91, pp. 55–63, 2016.

[54] K. R. Brodkin, A. J. García, and M. E. Levenston, “Chondrocyte phenotypes on different extracellular matrix monolayers,” *Biomaterials*, vol. 25, no. 28, pp. 5929–5938, 2004.

[55] M. Hamaji, F. Kojima, S. Koyasu, T. Tsuruyama, T. Komatsu, T. Ikuno, H. Date, and T. Nakamura, “Development of a composite and vascularized tracheal scaffold in the omentum for in situ tissue engineering: A canine model,” *Interact. Cardiovasc. Thorac. Surg.*, vol. 19, no. 3, pp. 357–362, 2014.

[56] S. K., A. W., M. Y., S. N., Y. Y., K. K., F. H., H. D.A., Y. H., and N. N., “Next Generation Mesenchymal Stem Cell (MSC)–Based Cartilage Repair Using Scaffold-Free Tissue Engineered Constructs Generated with Synovial Mesenchymal Stem Cells,” *Cartilage*, vol. 6, pp. 13–29, 2015.

[57] W. S. Toh, E. H. Lee, and T. Cao, “Potential of Human Embryonic Stem Cells in Cartilage Tissue Engineering and Regenerative Medicine,” *Stem Cell Rev. Reports*, vol. 7, no. 3, pp. 544–559, 2011.

[58] N. S. Hwang, S. Varghese, and J. Elisseeff, “Derivation of chondrogenically-committed cells from human embryonic cells for cartilage tissue regeneration,” *PLoS One*, vol. 3, no. 6, 2008.

[59] K. Takahashi and S. Yamanaka, “Induction of Pluripotent Stem Cells from Mouse Embryonic and Adult Fibroblast Cultures by Defined Factors,” *Cell*, vol. 126, no. 4, pp. 663–676, 2006.

[60] A. Inui, T. Iwakura, and a H. Reddi, “Human stem cells and articular cartilage regeneration,” *Cells*, vol. 1, no. 4, pp. 994–1009, Nov. 2012.

[61] A. P. Wong, S. Chin, S. Xia, J. Garner, C. E. Bear, and J. Rossant, “Efficient generation of functional CFTR-expressing airway epithelial cells from human pluripotent stem cells.,” *Nat. Protoc.*, vol. 10, no. 3, pp. 363–81, 2015.

[62] E. L. Rawlins and B. L. M. Hogan, “Ciliated epithelial cell lifespan in the mouse trachea and lung.,” *Am. J. Physiol. Lung Cell. Mol. Physiol.*, vol. 295, no. May 2008, pp. L231–L234, 2008.

[63] P. Macchiarini, M. Birchall, A. Hollander, S. Mantero, and M. Conconi, “Clinical transplantation of a tissue-engineered airway – Authors’ reply,” *Lancet*, vol. 373, no. 9665, pp. 718–719, Feb. 2009.

[64] C. R. Butler, R. E. Hynds, K. H. C. Gowers, D. D. H. Lee, J. M. Brown, C.

Crowley, V. H. Teixeira, C. M. Smith, L. Urbani, N. J. Hamilton, R. M. Thakrar, H. L. Booth, M. A. Birchall, P. De Coppi, A. Giangreco, C. O'Callaghan, and S. M. Janes, "Rapid expansion of human epithelial stem cells suitable for airway tissue engineering," *Am. J. Respir. Crit. Care Med.*, vol. 194, no. 2, pp. 156–168, 2016.

[65] K. Kobayashi, Y. Nomoto, T. Suzuki, Y. Tada, M. Miyake, A. Hazama, S. Kanemaru, T. Nakamura, and K. Omori, "Effect of fibroblasts on tracheal epithelial regeneration in vitro.," *Tissue Eng.*, vol. 12, no. 9, pp. 2619–28, 2006.

[66] M. Yamaya, W. E. Finkbeiner, S. Y. Chun, and J. H. Widdicombe, "Differentiated structure and function of cultures from human tracheal epithelium.," *Am. J. Physiol.*, vol. 262, no. 6 Pt 1, pp. L713-24, 1992.

[67] M. L. Fulcher and S. H. Randell, "Human nasal and tracheo-bronchial respiratory epithelial cell culture.," *Methods Mol. Biol.*, vol. 945, pp. 109–21, 2013.

[68] G. Tani, N. Usui, M. Kamiyama, T. Oue, and M. Fukuzawa, "In vitro construction of scaffold-free cylindrical cartilage using cell sheet-based tissue engineering," *Pediatr. Surg. Int.*, vol. 26, pp. 179–185, 2010.

[69] D. A. Gilpin, M. S. Weidenbecher, and J. E. Dennis, "Scaffold-free tissue-engineered cartilage implants for laryngotracheal reconstruction," *Laryngoscope*, vol. 120, no. 3, pp. 612–617, 2010.

[70] M. Weidenbecher, H. M. Tucker, A. Awadallah, and J. E. Dennis, "Fabrication of a neotrachea using engineered cartilage.," *Laryngoscope*, vol. 118, no. April, pp. 593–598, 2008.

[71] G. A. Whitney, H. Mera, M. Weidenbecher, A. Awadallah, J. M. Mansour, and J. E. Dennis, “Methods for producing scaffold-free engineered cartilage sheets from auricular and articular chondrocyte cell sources and attachment to porous tantalum.,” *Biores. Open Access*, vol. 1, no. 4, pp. 157–65, 2012.

[72] P. Jungebluth, A. Bader, S. Baiguera, S. Möller, M. Jaus, M. L. Lim, K. Fried, K. R. Kjartansdóttir, T. Go, H. Nave, W. Harringer, V. Lundin, A. I. Teixeira, and P. Macchiarini, “The concept of in vivo airway tissue engineering,” *Biomaterials*, vol. 33, no. 17, pp. 4319–4326, 2012.

[73] A. D. Dikina, H. A. Strobel, B. P. Lai, M. W. Rolle, and E. Alsberg, “Engineered cartilaginous tubes for tracheal tissue replacement via self-assembly and fusion of human mesenchymal stem cell constructs,” *Biomaterials*, vol. 52, no. 1, pp. 452–462, Jun. 2015.

[74] C. Del Gaudio, S. Baiguera, M. Boieri, B. Mazzanti, D. Ribatti, A. Bianco, and P. Macchiarini, “Induction of angiogenesis using VEGF releasing genipin-crosslinked electrospun gelatin mats,” *Biomaterials*, vol. 34, no. 31, pp. 7754–7765, 2013.

[75] M. Komura, H. Komura, K. Konishi, T. Ishimaru, K. Hoshi, T. Takato, Y. Tabata, and T. Iwanaka, “Promotion of tracheal cartilage growth by intra-tracheal injection of basic fibroblast growth factor (b-FGF),” *J. Pediatr. Surg.*, vol. 49, no. 2, pp. 296–300, 2014.

[76] A. Tani, Y. Tada, T. Takezawa, M. Imaizumi, Y. Nomoto, T. Nakamura, and K. Omori, “Regeneration of tracheal epithelium using a collagen vitrigel-sponge scaffold containing basic fibroblast growth factor,” *Ann. Otol. Rhinol. Laryngol.*,

vol. 121, no. 4, pp. 261–268, 2012.

[77] L. M. Ott, C. H. Vu, A. L. Farris, K. D. Fox, R. a. Galbraith, M. L. Weiss, R. a. Weatherly, and M. S. Detamore, “Functional Reconstruction of Tracheal Defects by Protein-Loaded, Cell-Seeded, Fibrous Constructs in Rabbits,” *Tissue Eng. Part A*, vol. 21, no. 17–18, pp. 2390–2403, 2015.

[78] C. Del Gaudio, S. Baiguera, F. Ajalloueian, A. Bianco, and P. Macchiarini, “Are synthetic scaffolds suitable for the development of clinical tissue-engineered tubular organs?,” *J. Biomed. Mater. Res. - Part A*, vol. 102, no. 7, pp. 2427–2447, Jul. 2014.

[79] K. H. Chua, B. S. Aminuddin, N. H. Fuzina, and B. H. I. Ruszymah, “Basic fibroblast growth factor with human serum supplementation: Enhancement of human chondrocyte proliferation and promotion of cartilage regeneration,” *Singapore Med. J.*, vol. 48, no. 4, pp. 324–332, 2007.

[80] B. D. Elder and K. A. Athanasiou, “Systematic assessment of growth factor treatment on biochemical and biomechanical properties of engineered articular cartilage constructs,” *Osteoarthr. Cartil.*, vol. 17, no. 1, pp. 114–123, 2009.

[81] J. Kim, S. W. Suh, J. Y. Shin, J. H. Kim, Y. S. Choi, and H. Kim, “Replacement of a tracheal defect with a tissue-engineered prosthesis: Early results from animal experiments,” *J. Thorac. Cardiovasc. Surg.*, vol. 128, no. 1, pp. 124–129, 2004.

[82] Q. Tan, R. Steiner, L. Yang, M. Welti, P. Neuenschwander, S. Hillinger, and W. Weder, “Accelerated angiogenesis by continuous medium flow with vascular endothelial growth factor inside tissue-engineered trachea.,” *Eur. J. Cardiothorac.*

Surg., vol. 31, no. 5, pp. 806–811, 2007.

[83] S. Haykal, M. Salna, Y. Zhou, P. Marcus, M. Fatehi, G. Frost, T. Machuca, S. O. P. Hofer, and T. K. Waddell, “Double-Chamber Rotating Bioreactor for Dynamic Perfusion Cell Seeding of Large-Segment Tracheal Allografts: Comparison to Conventional Static Methods.,” *Tissue Eng. Part C. Methods*, vol. 20, no. 8, pp. 1–12, 2014.

[84] G. Vunjak-Novakovic, I. Martin, B. Obradovic, S. Treppo, A. J. Grodzinsky, R. Langer, and L. E. Freed, “Bioreactor cultivation conditions modulate the composition and mechanical properties of tissue-engineered cartilage,” *J. Orthop. Res.*, vol. 17, no. 1, pp. 130–138, 1999.

[85] A. Bader and P. Macchiarini, “Moving towards in situ tracheal regeneration: the bionic tissue engineered transplantation approach,” *J. Cell. Mol. Med.*, vol. 14, no. 7, pp. 1877–1889, 2010.

[86] M. A. Asnaghi, P. Jungebluth, M. T. Raimondi, S. C. Dickinson, L. E. N. Rees, T. Go, T. a. Cogan, A. Dodson, P. P. Parnigotto, A. P. Hollander, M. a. Birchall, M. T. Conconi, P. Macchiarini, and S. Mantero, “A double-chamber rotating bioreactor for the development of tissue-engineered hollow organs: From concept to clinical trial,” *Biomaterials*, vol. 30, no. 29, pp. 5260–5269, 2009.

[87] Q. Tan, S. Hillinger, C. a van Blitterswijk, and W. Weder, “Intra-scaffold continuous medium flow combines chondrocyte seeding and culture systems for tissue engineered trachea construction.,” *Interact. Cardiovasc. Thorac. Surg.*, vol. 8, no. 1, pp. 27–30, 2009.

[88] C. H. Lin, S. hui Hsu, C. E. Huang, W. T. Cheng, and J. M. Su, “A scaffold-bioreactor system for a tissue-engineered trachea,” *Biomaterials*, vol. 30, no. 25, pp. 4117–4126, 2009.

[89] T. Go, P. Jungebluth, S. Baiguero, A. Asnaghi, J. Martorell, H. Ostertag, S. Mantero, M. Birchall, A. Bader, and P. Macchiarini, “Both epithelial cells and mesenchymal stem cell-derived chondrocytes contribute to the survival of tissue-engineered airway transplants in pigs,” *J. Thorac. Cardiovasc. Surg.*, vol. 139, no. 2, pp. 437–443, 2010.

[90] B. H. I. Ruszymah, K. Chua, M. A. Latif, F. Nor Hussein, and A. Bin Saim, “Formation of in vivo tissue engineered human hyaline cartilage in the shape of a trachea with internal support,” *Int. J. Pediatr. Otorhinolaryngol.*, vol. 69, no. 11, pp. 1489–1495, 2005.

[91] B. B. Mishell and S. M. Shiigi, *Selected Methods in Cellular Immunology*. W.H. Freeman and Company, 1980.

[92] D. H. Hoch, a J. Grodzinsky, T. J. Koob, M. L. Albert, and D. R. Eyre, “Early changes in material properties of rabbit articular cartilage after meniscectomy.,” *J. Orthop. Res.*, vol. 1, no. 1, pp. 4–12, 1983.

[93] Y. J. Kim, R. L. Y. Sah, J. Y. H. Doong, and A. J. Grodzinsky, “Fluorometric assay of DNA in cartilage explants using Hoechst 33258,” *Anal. Biochem.*, vol. 174, no. 1, pp. 168–176, Oct. 1988.

[94] R. W. Farndale, D. J. Buttle, and A. J. Barrett, “Improved quantitation and discrimination of sulphated glycosaminoglycans by use of dimethylmethylene

blue," *BBA - Gen. Subj.*, vol. 883, no. 2, pp. 173–177, Sep. 1986.

[95] R. L. Goldberg and L. M. Kolibas, "An Improved Method for Determining Proteoglycans Synthesized by Chondrocytes in Culture," *Connect. Tissue Res.*, vol. 24, no. 3–4, pp. 265–275, Jan. 1990.

[96] J. F. Woessner, "The determination of hydroxyproline in tissue and protein samples containing small proportions of this imino acid," *Arch. Biochem. Biophys.*, vol. 93, no. 2, pp. 440–447, May 1961.

[97] Z. Li, W. Hou, and D. Bromme, "Collagenolytic Activity of Cathepsin K Is Specifically Modulated by Cartilage-Resident Chondroitin Sulfates," *Biochemistry*, vol 39, no. 3, pp. 529–536, 2000.

[98] J. Kreuter, "Nanoparticles and microparticles for drug and vaccine delivery.," *J. Anat.*, vol. 189, no. 3, pp. 503–505, 1996.

[99] B. Hoffman, M. Martin, B. N. Brown, L. J. Bonassar, and J. Cheetham, "Biomechanical and biochemical characterization of porcine tracheal cartilage," *Laryngoscope*, vol. 126, no. 10, pp. E325–E331, 2016.

[100] P. Das, D. J. Schurman, L. Smith, and R. L. Smith, "Nitric oxide and G proteins mediate the response of bovine articular chondrocytes to fluid-induced shear," *J. Orthop. Res.*, vol. 15, no. 1, pp. 87–93, 1997.

[101] R. L. Smith, B. S. Donlon, M. K. Gupta, M. Mohtai, P. Das, D. R. Carter, J. Cooke, G. Gibbons, N. Hutchinson, and D. J. Schurman, "Effects of fluid-induced shear on articular chondrocyte morphology and metabolism in vitro," *J. Orthop. Res.*,

vol. 13, no. 6, pp. 824–831, 1995.

[102] H. Apparatus, “InBreath Bioreactor: Operator’s Manual.” pp. 1–24, 2013.

[103] S. M. Kunisaki, D. A. Freedman, and D. O. Fauza, “Fetal tracheal reconstruction with cartilaginous grafts engineered from mesenchymal amniocytes,” *J. Pediatr. Surg.*, vol. 41, no. 4, pp. 675–682, 2006.

[104] V. C. Mow, W. Zhu, and A. Ratcliffe, “Structure and function of articular cartilage and meniscus,” *Basic Orthop. Biomech. Raven Press. New York.*, pp. 143–145, 1991.

[105] L. M. Ott, T. A. Zabel, N. K. Walker, A. L. Farris, J. T. Chakroff, D. G. Ohst, J. K. Johnson, S. H. Gehrke, R. A. Weatherly, and M. S. Detamore, “Mechanical evaluation of gradient electrospun scaffolds with 3D printed ring reinforcements for tracheal defect repair.,” *Biomed. Mater.*, vol. 11, no. 2, p. 25020, 2016.

[106] G. Sommer, P. Regitnig, L. Költringer, G. a Holzapfel, L. Koltringer, and G. a Holzapfel, “Biaxial mechanical properties of intact and layer-dissected human carotid arteries at physiological and supraphysiological loadings.,” *Am. J. Physiol. Heart Circ. Physiol.*, vol. 298, no. 3, pp. H898–H912, 2010.

[107] G. D. DuRaine, W. E. Brown, J. C. Hu, and K. A. Athanasiou, “Emergence of Scaffold-Free Approaches for Tissue Engineering Musculoskeletal Cartilages,” *Ann. Biomed. Eng.*, vol. 43, no. 3, pp. 543–554, 2015.

[108] D. J. Responte, B. Arzi, R. M. Natoli, J. C. Hu, and K. A. Athanasiou, “Mechanisms underlying the synergistic enhancement of self-assembled

neocartilage treated with chondroitinase-ABC and TGF-??1," *Biomaterials*, vol. 33, no. 11, pp. 3187–3194, 2012.

[109] R. M. Natoli, C. M. Revell, and K. A. Athanasiou, "Chondroitinase ABC treatment results in greater tensile properties of self-assembled tissue-engineered articular cartilage.," *Tissue Eng. Part A*, vol. 15, no. 10, pp. 3119–28, 2009.

[110] E. A. Makris, R. F. MacBarb, N. K. Paschos, J. C. Hu, and K. A. Athanasiou, "Combined use of chondroitinase-ABC, TGF-??1, and collagen crosslinking agent lysyl oxidase to engineer functional neotissues for fibrocartilage repair," *Biomaterials*, vol. 35, no. 25, pp. 6787–6796, 2014.

[111] P. D. Benya and J. D. Shaffer, "Dedifferentiated chondrocytes reexpress the differentiated collagen phenotype when cultured in agarose gels," *Cell*, vol. 30, no. 1, pp. 215–224, 1982.

[112] G. Schulze-Tanzil, P. De Souza, H. Villegas Castrejon, T. John, H. J. Merker, A. Scheid, and M. Shakibaei, "Redifferentiation of dedifferentiated human chondrocytes in high-density cultures," *Cell Tissue Res.*, vol. 308, no. 3, pp. 371–379, 2002.

[113] E. M. Darling and K. A. Athanasiou, "Rapid phenotypic changes in passaged articular chondrocyte subpopulations," *J. Orthop. Res.*, vol. 23, no. 2, pp. 425–432, 2005.

[114] H. K. Heywood, G. Nalesso, D. a Lee, and F. Dell'accio, "Culture expansion in low-glucose conditions preserves chondrocyte differentiation and enhances their subsequent capacity to form cartilage tissue in three-dimensional culture.," *Biores.*

Open Access, vol. 3, no. 1, pp. 9–18, 2014.

[115] K. M. Hubka, R. L. Dahlin, V. V Meretoja, K. Kasper, and A. G. Mikos, “Enhancing Chondrogenic Phenotype for Cartilage Tissue Engineering: Monoculture and Co-culture of Articular Chondrocytes and Mesenchymal Stem Cells,” *Tissue Eng. Part B*, vol. 20, no. 6, pp. 1–50, 2014.

[116] D. a Lee, T. Reisler, and D. L. Bader, “Expansion of chondrocytes for tissue engineering in alginate beads enhances chondrocytic phenotype compared to conventional monolayer techniques.,” *Acta Orthop. Scand.*, vol. 74, no. 1, pp. 6–15, 2003.

[117] T. Fong Ng, M. Matmati, and T. M. Quinn, “Protection of the Differentiated Chondrocyte Phenotype during Monolayer Expansion Cultures Using Heat Inactivated Fetal Calf Serum,” *McGill Sci. Undergrad. Res. J.*, vol. 7, no. 1, pp. 42–48, 2012.